

Structural prototypes for an extended family of flavoprotein reductases: Comparison of phthalate dioxygenase reductase with ferredoxin reductase and ferredoxin



CARL C. CORRELL,^{1,3} MARTHA L. LUDWIG,¹ CHRISTOPHER M. BRUNS,² AND P. ANDREW KARPLUS²

¹ Department of Biological Chemistry and Biophysics Research Division,
University of Michigan, Ann Arbor, Michigan 48109

² Division of Biological Sciences, Section of Biochemistry, Molecular and Cell Biology,
Cornell University, Ithaca, New York 14853

(RECEIVED May 28, 1993; ACCEPTED September 7, 1993)

Abstract

The structure of phthalate dioxygenase reductase (PDR), a monomeric iron-sulfur flavoprotein that delivers electrons from NADH to phthalate dioxygenase, is compared to ferredoxin-NADP⁺ reductase (FNR) and ferredoxin, the proteins that reduce NADP⁺ in the final reaction of photosystem I. The folding patterns of the domains that bind flavin, NAD(P), and [2Fe-2S] are very similar in the two systems. Alignment of the X-ray structures of PDR and FNR substantiates the assignment of features that characterize a family of flavoprotein reductases whose members include cytochrome P-450 reductase, sulfite and nitrate reductases, and nitric oxide synthase. Hallmarks of this subfamily of flavoproteins, here termed the FNR family, are an antiparallel β -barrel that binds the flavin prosthetic group, and a characteristic variant of the classic pyridine nucleotide-binding fold. Despite the similarities between FNR and PDR, attempts to model the structure of a dissociable FNR:ferredoxin complex by analogy with PDR reveal features that are at odds with chemical crosslinking studies (Zanetti, G., Morelli, D., Ronchi, S., Negri, A., Aliverti, A., & Curti, B., 1988, *Biochemistry* 27, 3753–3759).

Differences in the binding sites for flavin and pyridine nucleotides determine the nucleotide specificities of FNR and PDR. The specificity of FNR for NADP⁺ arises primarily from substitutions in FNR that favor interactions with the 2' phosphate of NADP⁺. Variations in the conformation and sequences of the loop adjoining the flavin phosphate affect the selectivity for FAD versus FMN.

The midpoint potentials for reduction of the flavin and [2Fe-2S] groups in PDR are higher than their counterparts in FNR and spinach ferredoxin, by about 120 mV and 260 mV, respectively. Comparisons of the structure of PDR with spinach FNR and with ferredoxin from *Anabaena 7120*, along with calculations of electrostatic potentials, suggest that local interactions, including hydrogen bonds, are the dominant contributors to these differences in potential.

Keywords: [2Fe-2S] cluster; flavin-binding site; oxidation-reduction potentials; protein evolution; pyridine nucleotide specificity

Reprint requests to: Martha L. Ludwig, Biophysics Research Division, University of Michigan, 930 North University Avenue, Room 3038, Ann Arbor, Michigan 48109-1055.

³ Present address: Department of Molecular Biophysics and Biochemistry, Yale University, New Haven, Connecticut 06520.

Abbreviations: PDR, phthalate dioxygenase reductase; FNR, ferredoxin-NADP⁺ reductase; GR, glutathione reductase; Fd, ferredoxin; HiPIP, high-potential iron protein; ox, sq, red, oxidized, semiquinone, and reduced states of flavins; 2e, two-electron; RMS, root mean square.

Comparisons of sequence alignments with the X-ray structure of spinach ferredoxin-NADP⁺ reductase (Karplus et al., 1991) have defined a family of flavin-dependent oxidoreductases whose best known members are FNR and cytochrome P-450 reductase. A pattern of conserved residues, located in the flavin and pyridine nucleotide-binding sites, was proposed by Karplus and coworkers (1991) to be the sequence signature characteristic of the family

(Fig. 1). The ordering of these binding sequences along the chain is important in discriminating FNR proteins from other families. The structural motif shared by all members of the family is expected to be a two-domain module resembling FNR, with one domain binding the flavin and the other binding pyridine nucleotide. We will refer to this unit as the "FNR-like module." Sequence alignments of several reductases (Neidle et al., 1991) and the structure determination of phthalate dioxygenase reductase (Correll et al., 1992) have subsequently related additional proteins to cytochrome P-450 reductase and FNR. The C-terminal sequence of nitric oxide synthase has been found to resemble cytochrome P-450 reductase (Bredt et al., 1991). Other alignments and identifications have been reported (Hyde et al., 1991; Andrews et al., 1992; Segal et al., 1992). In this paper, comparisons of FNR and PDR are used in a further evaluation of the distinguishing traits of the FNR family.

The shared function of the proteins in the FNR family is flavin-dependent conversion between two-electron reactions with pyridine nucleotides and one-electron reactions with carriers (Table 1), although the pathways of electron transfer remain to be established for some members of the family. The one-electron carriers are sometimes independent proteins, but in most cases are found in domains fused to the N- or C-terminus of the fundamental FNR-like module (Table 1). FNR and cytochrome b_5 reductase, each with just two domains, are representative of the simplest structures in the group and react with dissociable carriers. At the next level of complexity are cytochrome P-450 reductase, sulfite reductase- α , and PDR, among others, in which a one-electron carrier domain is fused to the two-domain core via linking sequences. The carriers in this group transfer electrons to cognate acceptors like cytochrome P-450. The most complicated structures, nitrate reductase and nitric oxide synthase, include additional sequences and prosthetic groups, indicating the presence of more than three structural domains.

The X-ray analysis of PDR (Correll et al., 1992), a protein in which a ferredoxin-like [2Fe-2S] domain is attached to the C-terminus of an FNR-like module, provides the first structural example of an interface between a carrier and an FNR-like module. In PDR the [2Fe-2S] cluster is situated close to the dimethylbenzene end of the flavin ring of FMN, with a minimum distance of 4.7 Å between atoms of the two prosthetic groups. The domain:domain interactions in PDR position the carrier moiety so that an acceptor dioxygenase can also approach the [2Fe-2S] cluster. We expect that one-electron carriers associated with other members of the FNR family will also bind near the protruding end of the flavin ring.

Despite the general structural similarities that relate the two proteins, FNR and PDR differ in their selectivities for the flavin and pyridine nucleotides: FNR binds FAD and is specific for NADP(H) as substrate, whereas PDR binds

FMN and is specific for NAD(H). Comparison of the structures of FNR and PDR reveals features that control these nucleotide specificities.

In PDR, as in most enzymes of the FNR family (Table 1), the direction of electron flow is from flavin to a one-electron acceptor or an electron transfer chain. FNR is an unusual case in which the physiological electron flow is in the opposite direction and the overall reaction produces NADPH. This functional difference is reflected in large variations in the flavin and carrier potentials, which for PDR and FNR must stem from differences in protein:flavin and protein:[2Fe-2S] interactions. The 2e midpoint potential for the flavin is about -350 mV in FNR (Keirns & Wang, 1972; Batie & Kamin, 1981; Pueyo et al., 1991), below the potential for pyridine nucleotides (ca. -320 mV), and the potential of Fd in the FNR:Fd complex is -430 to -500 mV, well below the flavin midpoint (Batie & Kamin, 1981; Pueyo et al., 1991). In contrast, the flavin midpoint potential is -230 mV in PDR, and the one-electron potential of [2Fe-2S] is even higher, at -174 mV (Batie et al., in prep.). The variations of potential in FNR:Fd and PDR correspond to an energy difference of 6.0 kcal/mol for two-electron reduction of the flavins and 7.5 kcal/mol for reduction of the [2Fe-2S] centers. Comparisons of protein:prosthetic group interactions in PDR with those in FNR and in the low potential [2Fe-2S] Fd from *Anabaena 7120* (Rypniewski et al., 1991), using refined structures (see Methods), reveal structural differences that contribute to the differences in potentials.

Results and discussion

Structural alignment of PDR with spinach FNR and *Anabaena* ferredoxin

The close structural similarity of FNR and PDR implies that these proteins are related by divergent evolution. Even though FNR and PDR share only 15% sequence identity, a core of 160 residues overlays in three dimensions with an RMS $C\alpha$ deviation of 1.52 Å. Within this core the sequence identity is 19%. Inspection of the overlaid structures (Fig. 2; Kinemage 1) reveals strong conservation of the β -sheet strands of the flavin and pyridine nucleotide-binding domains and of the domain-domain packing. If the two domains are overlaid separately, the optimal rotations differ by less than 6°. In two segments of the pyridine nucleotide-binding domain, FNR has pairs of α -helices ($N\alpha 3$, $N\alpha 3'$ and $N\alpha 4$, $N\alpha 4'$) connecting β -strands whereas PDR has single helices ($N\alpha 3$ and $N\alpha 4$). In these regions neither of the FNR helices corresponds well with the PDR helices, so residues in these segments are not considered to be structurally equivalent except at the start of $N\alpha 4$ (see Fig. 2B). As is common, the positions of the helices are less well conserved than the β -sheets, and helices are shifted and rotated by as much as 3 Å and 20°. The observed shifts are close to those

	1	2	3	4	5	6
PDR:	55^{RTYS}	80^{RGGS}	120^{GIGITP}	173^{DH}	197^{YCCGP}	223^{ESF}
FNR:	93^{RLYS}	130^{GVCS}	171^{GTGIAP}	234^{SR}	270^{YMCGL}	312^{EVY}
Consensus:	rx_{FT}^{YS}	Gxx_T^S_(FAD)	GtGixp	sr_(NADP)	yxcGp	exf
		RGGS_(FMN)			de_(NAD)	

Fig. 1. Conserved sequences that characterize the FNR family. Well-conserved “fingerprint” sequence regions in PDR and FNR are aligned in lines 1 and 2. Bold characters represent residues implicated in binding flavin or pyridine nucleotides. Line 3 presents an approximate consensus sequence for the whole family. Here, uppercase characters represent absolutely conserved residues and two stacked uppercase characters indicate positions where only two residues seem to be allowed. The first and second sequences bind the isoalloxazine and phosphate groups of the flavin, respectively. The consensus for segment 2 distinguishes FAD- and FMN-binding members of the family. Because sequences are available for only two known FMN-binding enzymes, the RGGS residues may not all be well conserved (see text). The third sequence is characteristic for the pyridine nucleotide diphosphate site and the fourth sequence distinguishes NAD⁺ and NADP⁺ specific proteins. Segment 4 is variable, especially in NAD⁺-specific proteins, most of which have an acidic residue in this region. The conserved C in the fifth sequence may be involved in binding the nicotinamide group (Shirabe et al., 1991; Aliverti et al., 1993). The final aromatic residue of the last sequence is stacked against the flavin ring. There are some additional well-conserved residues in portions of the sequence not shown here, including an absolutely conserved glycine at 42_{PDR} and 73_{FNR}. However, these other residues have not been implicated in enzyme function.

Table 1. The FNR electron transferase family: Domain arrangements and functional specificity^a

Reductase	Domain structure	E_o flavin (pH)	E_o carrier (pH)	References, comments
FNR				
Spinach	N-[FAD-NADP]-C	−377 (2e) (8.0) [−347 (7.0)] ^b	−420 (8.4)	Batie & Kamin (1984), Karplus et al.* (1984)
Spinach <i>Anabaena</i>		−445 ^c (2e) (9.0) −344 ^d (2e) (7.0)	−505 ^c (9.0)	Batie & Kamin (1981) Pueyo et al. (1991)
B5R: Liver	N-[FAD-NAD]-C	−258 (2e) (7.0)	0–13	Iyanagi (1977), Tomatsu et al.* (1989)
PDR: <i>Pseudomonas cepacia</i>	N-[FMN-NAD]-[2Fe-2S]-C	−174, −284 (7.0)	−174 (7.0)	Liu & Zylstra* (1992), Ballou (pers. comm.)
MMO-C: <i>Methylococcus capsulatus</i>	N-[2Fe-2S]-[FAD-NAD]-C	−150, −260 (7.0)	−220 (7.0)	Lund & Dalton (1985), Stainthorpe* et al. (1990)
P450R: microsomal	N-[FMN]-[FAD'-NADP]-C	−290, −365 (7.0)	−110, −270 (7.0)	Iyanagi et al. (1974), Haniu* et al. (1989), Ostrowski* (1989)
SR-α: <i>Escherichia coli</i>	N-[FMN]-[FAD'-NADP]-C	−382, −322 (7.7)	−152, −327 (7.7)	Spence et al. (1988), Kay et al. (1989), Prosser et al.* (1990)
NR: Spinach	N-[P]-[Cyt b]-[FAD-NAD]-C	−280 ^e (2e, 7.0)	−123, −172 (7.0)	

^a Data are tabulated for the best characterized members of the family for which redox potentials have also been determined. FNR and PDR are the only enzymes for which X-ray structures are published. The domain organization was deduced from the sequences and alignments, as indicated in the starred (*) references. Nucleotide specificities are indicated in the drawings describing domain organization. Of the seven reductases, FNR is unique in catalyzing the reduction of pyridine nucleotide, but the other proteins display considerable variation in the potentials of their flavin prosthetic groups. Abbreviations: B5R, NADH-cytochrome *b*₅ reductase; MMO-C, methane monooxygenase component C; NR, nitrate reductase; P450R, cytochrome P-450 reductase; SR-α, sulfite reductase component α. FAD' indicates that sequences suggest a large insert in the FAD domain, relative to FNR. [P] refers to a pterin-binding moiety. Other proteins identified as members of the family (Neidle et al., 1991; Andrews et al., 1992) are xylene monooxygenase reductase (Suzuki et al., 1991), toluate dioxygenase reductase (XylZ) (Neidle et al., 1991), vanillate demethylase reductase (Brunel & Davison, 1988), benzoate dioxygenase reductase (Neidle et al., 1991), naphthalene dioxygenase ferredoxin reductase (Simon et al., 1993), nitric oxide synthase (Bredt et al., 1991), bacterial hemoglobin-like protein (HMP) (Andrews et al., 1992), LuxG (Swartzman et al., 1990), ferrisiderophore reductase C (Fsrc) (Spyrou et al., 1991; Andrews et al., 1992), phenol hydroxylase component 5 (Nordlund et al., 1990), and cytochrome *b*₂₄₅ (Segal et al., 1992).

^b Calculated from pH 8.0 measurement.

^c Determined in the FNR:Fd complex.

^d The ox/sq potential is approximately −370; the sq/red potential is approximately −320.

^e The potentials shift when pyridine nucleotides are bound.

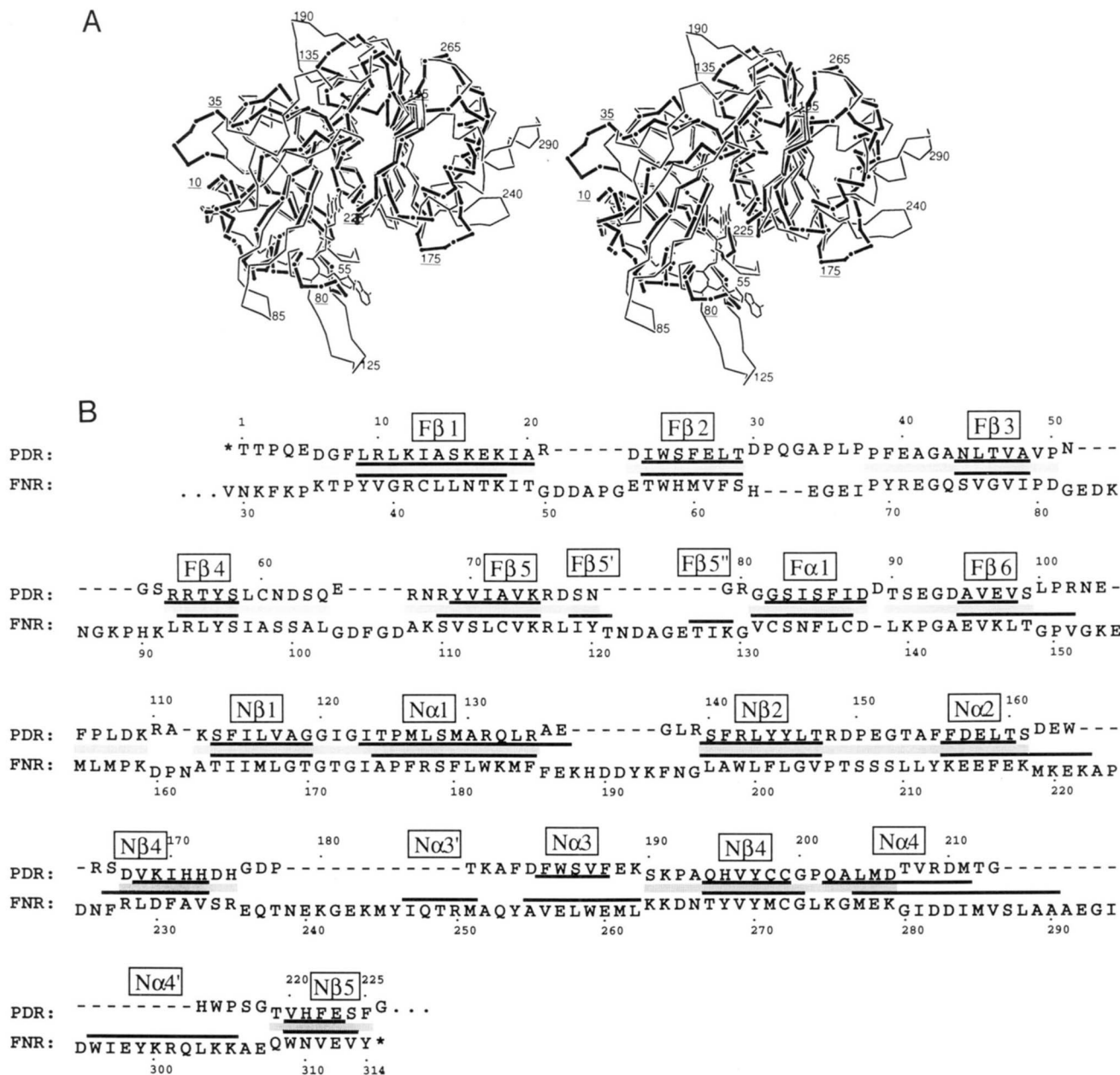


Fig. 2. **A:** Superposition of the FNR and PDR structures. A C α representation of FNR (thin lines) overlaid on the FMN and NAD domains of PDR (thick lines) with the FAD from FNR included. Underlined labels designate PDR residues. The topologies of the flavin and pyridine nucleotide-binding domains are the same in both proteins. The N-terminal flavin domains are six-stranded barrels with sheet topology 1, 3, -1, -1, 3; the NAD(P) domains incorporate parallel β -sheets with the topology 1x, 1x, -3x, -1x. The two structures were superimposed by iterative rigid body least-squares minimization of the distances separating equivalent main-chain atoms (Kabsch, 1976), using only atomic separations of less than 3.0 Å (see Methods). **B:** Alignment of PDR with spinach FNR. The sequence alignment is based on the superposition of the three-dimensional structures. The PDR sequence numbering is shown above each set of sequences and FNR numbering is below. The sequence for PDR shown here is deduced from the DNA sequence of Liu and Zylstra (1992) and corresponds to the entry 2PIA in the Protein Data Bank. Regions where the structures are equivalent (see Methods) are indicated by gray bars and closer spacing of the sequences, whereas inserts and structural differences are observed in sequences that are spaced farther apart. Residues outside of the equivalent segments are aligned by approximate spatial proximity, and to improve alignment with homologous sequences. However, the residues aligned in these regions should *not* be considered structurally equivalent. Gaps, indicated by hyphens, are positioned to optimize proximity of the aligned residues. Residues inserted in FNR are at the N-terminus, which is partly disordered (Karplus et al., 1991), and at 51-55, 83-89, 103-106, 121-128, 188-193, 222-225, 239-250, and 287-302. Secondary structure elements (Kabsch & Sander, 1983) are indicated in each sequence by heavy black lines; the helical (α) and sheet (β) sequences are designated according to the labels in boxes, with "F" or "N" indicating whether they are in the flavin or the NAD(P) domain. FNR has two additional hairpin strands (F β 5' and F β 5'') and two additional helices, not found in PDR, which are labeled N α 3' and N α 4'.

expected from the level of divergence of FNR and PDR (Chothia & Lesk, 1986).

The flavin and pyridine nucleotide domains comprise all 314 residues of FNR but only the first 225 residues of PDR. Figure 2 shows that the additional 89 residues of FNR are inserted at the N-terminus, in eight external loops, and in the two helices, $\text{N}\alpha 3'$ and $\text{N}\alpha 4'$. The longest insertions into the FNR chain begin at residues 83, 121, 188, 239, and 287. Two of these, beginning at residues 121_{FNR} and 236_{FNR}, contribute to the selective binding of FAD (as opposed to FMN) and NADP⁺ (as opposed to NAD⁺). Because of the many insertions and small num-

ber of identities (only 30 residues in the conserved core), accurate alignment of the sequences would have been impossible without the structural information.

The [2Fe-2S] domain of PDR, residues 237–321, was superimposed on *Anabaena* 7120 ferredoxin using the backbone atoms of 81 equivalent residues. The three-dimensional superposition is displayed in Figure 3A and Kinemage 2, and Figure 3B shows the corresponding alignment of the primary sequences. The major differences in the folds are the extension of a hairpin near the N-terminus of Fd, and the presence of seven additional residues in an irregular helix at the C-terminus of Fd. Oth-

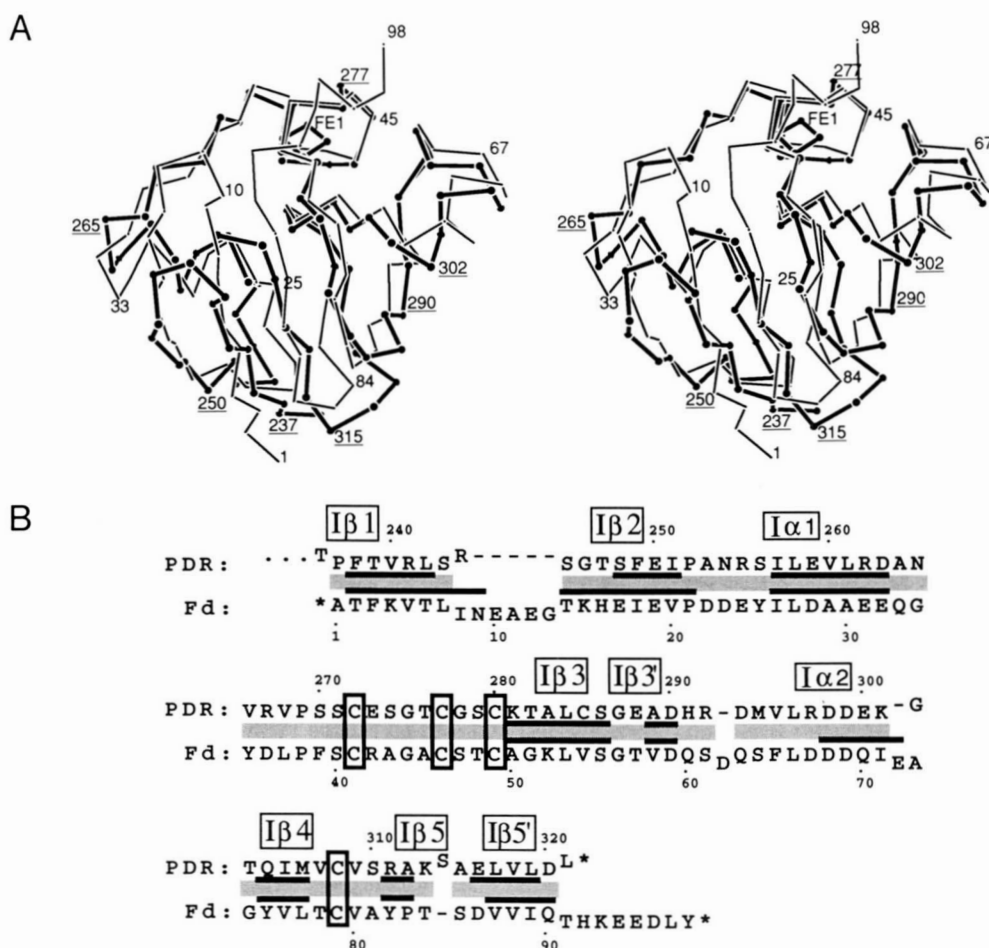


Fig. 3. **A:** Superposition of the [2Fe-2S] domain of PDR on *Anabaena* ferredoxin. The structures were overlaid as described in Figure 2, using backbone atoms from the 81 residues considered to be equivalent in panel B (RMS deviation = 1.9 Å). The orientation is the same as in Figure 2A. Although the initial hairpins of the two structures do not coincide well in space, the turns at 10–11 of Fd and 243–244 of PDR adopt related conformations with Gly 13_{Fd} and Gly 246_{PDR} in congruent positions. Gaps or inserts of single residues are found at three positions, and the seven terminal residues of Fd are missing from PDR. The C-terminal segment of Fd looks helical but is not defined as a helix by DSSP (cf. panel B). **B:** Alignment of the sequence of *Anabaena* Fd with residues 236–321 of PDR. Sequence alignments, based on superposition of the structures, were determined as described in Methods and in the legend of Figure 2. Secondary structure assignments were from DSSP (Kabsch & Sander, 1983), which finds a helix at residues 68–72 in Fd, but not at the corresponding residues, 298–302, in PDR. The elements of secondary structure are labeled I to denote the iron-sulfur domain, as in Correll et al. (1992). Cysteine residues that bind iron are shown in boxes. The photosynthetic Fd from *Anabaena* 7120 and the [2Fe-2S] domain of PDR vary in composition, with only 20 identities in the aligned regions of Figure 3B. Most notable are the differences in the number of aromatic residues, eight in Fd and two in PDR.

erwise the backbones conform closely, with only three gaps or insertions of single residues, at 292, 301, and 313 of PDR. In PDR the iron ligand Cys 280 is near the surface of the domain whereas in Fd the C-terminus shields the corresponding residue of the [2Fe-2S] cluster.

PDR provides the only structurally characterized example of an interface between a carrier domain and an FNR-like module. The accessible area buried in the interface, about 700 \AA^2 for each partner, is less than the area of $1,100 \text{ \AA}^2$ in the FMN:NAD domain-domain interface, and the interactions are reminiscent of protein-protein recognition sites or oligomer interfaces (Janin et al., 1988; Janin & Chothia, 1990) rather than domain-domain interfaces. The contacts between the [2Fe-2S] domain and the FNR-like module in PDR are relatively hydrophilic (more than 50% polar) and involve primarily side chain and through water interactions rather than main chain interactions (Fig. 4; Kinemage 3). Protein-protein interactions are typically mediated by hydrogen bonds and solvent bridges (Janin & Chothia, 1990). The concentration of Arg residues, remarkable in the PDR interface, has been noted in monomer-monomer interfaces (Janin et al., 1988). The properties of the FNR-module:[2Fe-2S] interface in PDR are consistent with evolutionary swap-

ping of the carrier domains. In contrast, the flavin:pyridine nucleotide domain interfaces in FNR and PDR are very hydrophobic, with only 30% of the buried surface comprised of polar residues.

Is PDR a model for the FNR:Fd complex?

PDR and the FNR:Fd complex both catalyze electron transfer between pyridine nucleotides and [2Fe-2S] centers, and the functionally related domains have equivalent folds, as shown in Figures 2 and 3. A putative model for FNR:Fd can be constructed by superposition of the structure of FNR on the equivalent domains of PDR and simultaneous superposition of *Anabaena* Fd on the [2Fe-2S] domain. In the resulting model, which is shown in Figure 5, some residues in helix I α 1 of Fd collide with the loop between F β 3 and F β 4 of FNR. Relaxations involving small rotations and translations of Fd or movement of the FNR loop at residues 84–92_{FNR} can relieve the bad contacts.

Interactions between FNR and Fd from spinach or other species have been examined by chemical modification (Zanetti et al., 1988), crosslinking (Vieira et al.,

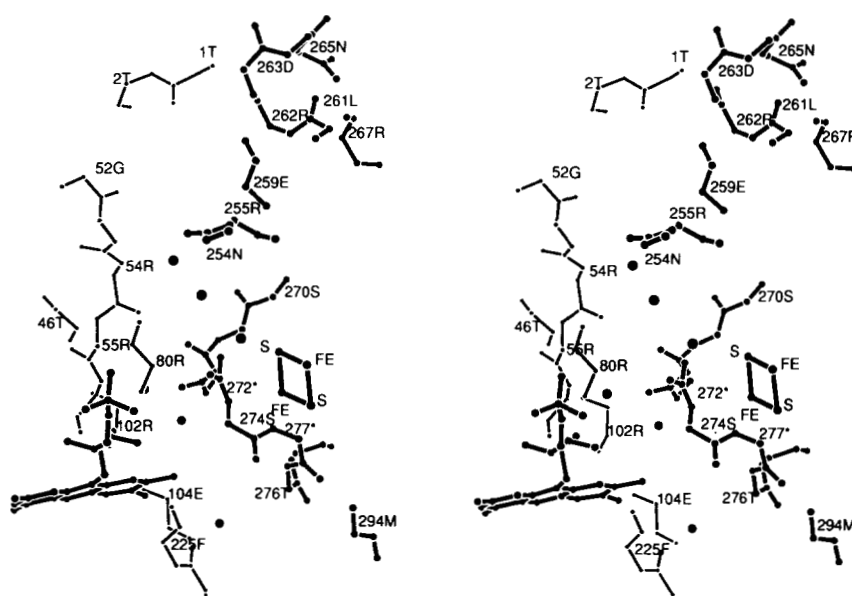


Fig. 4. Contacts between the [2Fe-2S] and the FNR-like domains of PDR. An edge-on view of the interface, showing the backbones of regions that contribute interface contacts. Residues from the [2Fe-2S] domain, at the right, are drawn with thicker bonds. Eight direct hydrogen bonds and six solvents (filled) connect the [2Fe-2S] domain to the FNR-like module. Cysteine ligands to iron are flagged with an asterisk. Segments of the FMN and NAD domains that contribute to the interface include residues 53 and 56, adjoining the flavin, and Arg 80 of the phosphate-binding loop, which are hydrogen bonded to Glu 259, Ser 271, Cys 272, and Glu 273. Side chains of Arg 102 and Asn 104, at the beginning of the FMN-NAD domain linker, participate in solvent-mediated contacts, and Thr 1 makes direct hydrogen bonds to Arg 262 and Asn 265. NAD-domain residues Gln 202 (not shown) and the segment 224–226 contact Thr 276 and Met 294, with a solvent connecting Ser 224 and Thr 276. The ribityl side chain of FMN contributes one direct and one bridging hydrogen bond to the interface contacts. The contacts from the [2Fe-2S] domain are dominated by the iron-sulfur loop at 271–280, which comprises almost 40% of the area from the [2Fe-2S] domain that is buried by contacts with the other domains. The other interface segments from the [2Fe-2S] domain, residues 259 and 262–267, and residues 292–294, lie on either side of the iron-sulfur loop.

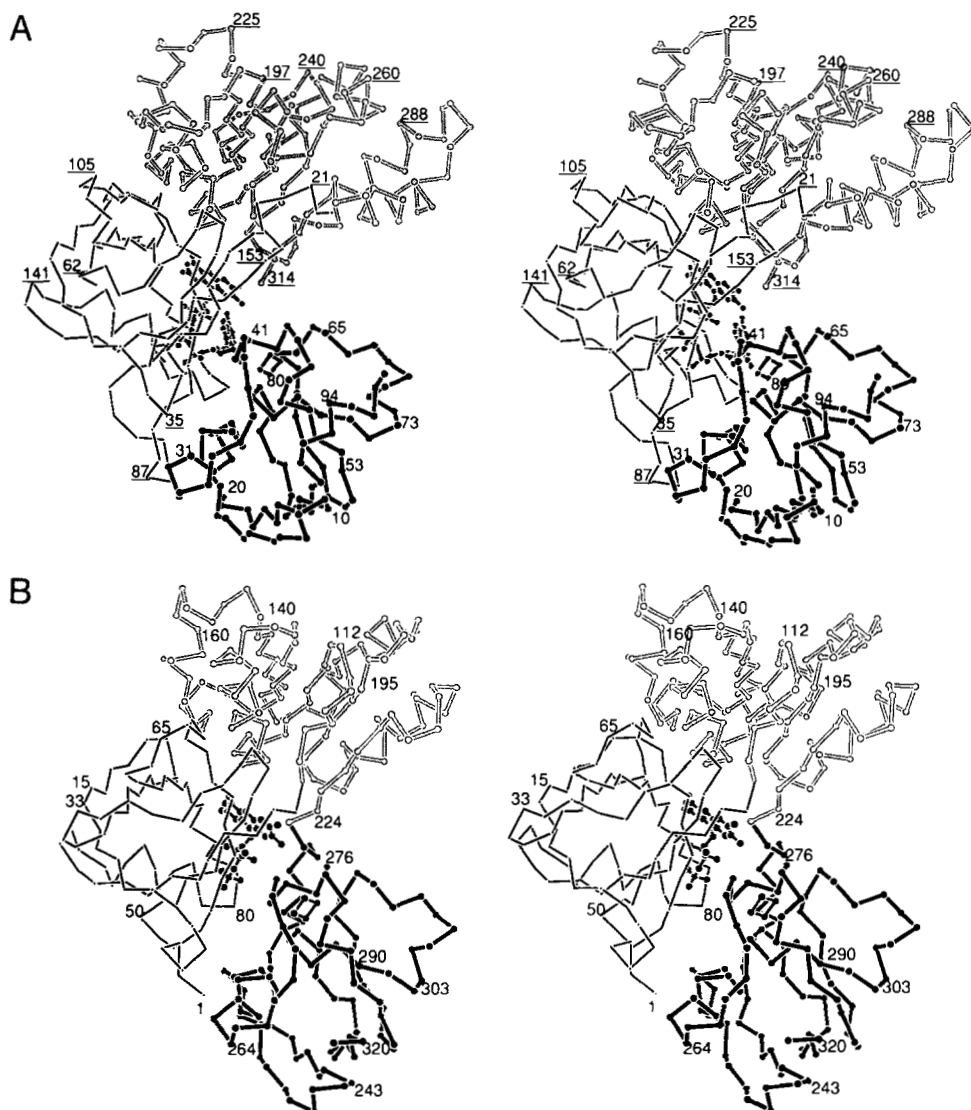


Fig. 5. A: An Fd:FNR model derived from the structure of PDR. The model was constructed by superimposing FNR on the FMN and NAD domains of PDR, and *Anabaena* Fd on the [2Fe-2S] domain of PDR. The domains of FNR are distinguished by thin and shaded bonds and residue numbers of FNR are underlined; Fd is represented by filled bonds. Some close contacts are evident in the model (see text). The view is rotated from Figure 2A to display the interface between Fd and FNR. *Anabaena* ferredoxin residues at the interface include Asp 28, Glu 32, residues 42–44 from the [2Fe-2S]-binding loop, and Ser 61. Residue 96, equivalent to Glu 94 that forms a crosslink in FNR:Fd (Zanetti et al., 1988), is not near the Fd:FNR interface in this model. **B:** A drawing of PDR in the same orientation as the model of Figure 5A.

1986; Zanetti et al., 1988; Pueyo et al., 1991, 1992), NMR (Chan et al., 1983), deletion analysis (Aliverti et al., 1990), and site-directed mutagenesis (Coghlan & Vickery, 1991; Hurley et al., 1993). Some of the Fd segments identified by these methods, e.g., the acidic residues of Fd near positions 25, 31, or 68, correspond approximately to regions of the [2Fe-2S] domain that participate in the PDR interface. However, the model complex depicted in Figure 5 is not consistent with the results of crosslinking (Vieira et al., 1986; Zanetti et al., 1988) or mutagenesis experiments (Hurley et al., 1993), which imply that the

C-terminus of Fd is near the FNR:Fd interface. The predominant crosslink in covalent complex(es) of spinach FNR:Fd connects the sequences near 85 in FNR with 83–95 in Fd, probably joining Glu 94 of spinach Fd (equivalent to Asp 96 of *Anabaena* ferredoxin) to Lys 85 or Lys 88 in FNR (Zanetti et al., 1988). However, in the model complex shown in Figure 5, the C-terminal region of Fd is on the outer surface, far from the interface, and the C α positions of Asp 96_{Fd} and Lys 85 or Lys 88_{FNR} are more than 25 Å apart. Models that place Asp 96_{Fd} close to Lys 88_{FNR} can be generated by rotating the

docked Fd molecule ca. 120–180° about an axis through the [2Fe–2S] cluster (Karplus, 1991; De Pascalis et al., 1993). Thus, the current evidence favors a different orientation for Fd in the FNR:Fd and PDR structures, despite the many parallels between the two systems.

Why might the FNR:Fd interface differ from the analogous interaction in PDR? In PDR and many other family members, this interface is formed within a single protein chain, while in FNR the interface is formed between two dissociable polypeptides. This distinction has both functional and structural consequences. Dissociable carriers such as plant Fds react independently with FNR and other redox centers and recognize a correct partner in each reaction. In contrast, covalently linked carriers such as the one in PDR must be able to react in situ with both the flavin of the FNR-like unit and another donor/acceptor. Thus, in PDR a crevice between the [2Fe–2S] and FMN domains allows phthalate dioxygenase to approach one side of the iron–sulfur cluster (near Cys 277) while the other side (near Cys 272) faces the flavin (Fig. 3A). The FNR:Fd interaction is free from this extra spatial constraint.

Flavin nucleotide binding and specificity in FNR and PDR

The riboflavin-binding sites are very similar in the FNR and PDR structures (Fig. 6). The protein and solvent-mediated interactions of sequences 55–58_{PDR} and 72–74_{PDR} with the isoalloxazine ring are equivalent to the interactions of 93–96 and 114–116 in FNR. Tyr 57_{PDR} and Tyr 95_{FNR} contact the *si* face of the flavin in each structure, and a conserved aromatic residue from the NAD(P) domain, Phe 225_{PDR} or Tyr 314_{FNR}, stacks against the *re* side of the flavin ring. Small differences in interatomic distances (see Methods) can affect the strength of hydrogen bonding to isoalloxazine atoms O(4) and N(5) (Fig. 6A; Kinemage 4; Table 2). For example, interactions of Ser 58_{PDR} and Ser 96_{FNR} differ slightly in the two structures, with the backbone NH of Ser 96_{FNR} closer to N(5) of the isoalloxazine and the NH of Ser 58_{PDR} closer to O(4).

FNR and PDR provide the first documented example of enzymes employing the same domain topology to bind both FMN and FAD. Most of the selectivity between

Table 2. Polar interactions of the FMN moieties in PDR and FNR^a

Flavin	FMN in PDR				FAD in FNR			
	Residue (atom)	Number	Distance (Å)	Angle (degrees)	Residue (atom)	Number	Distance (Å)	Angle (degrees)
O(2)	Lys(N)	74	3.0	162	Lys(N)	116	3.0	175
	Wat(O)	331	2.8		Wat(O)	410	2.7	
N(3)	Ala(O)	72	2.9	157	Cys(O)	114	2.8	159
	Ser(N)	58	3.3	157	Ser(N)	96	3.5	134
O(4)	Thr(OG1)	124	2.9	116	Wat(O)	403	3.1	
	Wat(O)	329	2.6		Wat(O)	409	2.9	
N(5)	Ser(N)	58	3.3	135	Ser(N)	96	3.2	154
O2*	Thr(O)	56	2.8	132	Leu(O)	94	2.8	141
	Wat(O)	332	2.7		Wat(O)	437	3.2	
O3*	Arg(NH2)	80	3.1	117			No equivalent	
	Ser(OG)	274	3.2	131			No equivalent	
	Wat(O)	354	3.1		Wat(O)	518	2.9	
O4*		No equivalent			Wat(O)	423	2.9	
	Wat(O)	331	2.6		Wat(O)	410	2.5	
	Tyr(OH)	57	3.6	103	Tyr(OH)	95	2.8	108
OP1	Ser(N)	83	3.2	158	Ser(N)	133	2.8	159
	Ser(OG)	83	2.8	99	Ser(OG)	133	2.3	113
	Wat(O)	327	2.6				No equivalent	
OP2	Gly(N)	82	2.8	129	Cys(N)	132	2.8	150
	Arg(NH2)	55	3.2	138	Arg(NH2)	93	3.3	131
	Arg(NE)	55	2.9	158	Arg(NE)	93	2.8	159
OP3	Arg(N)	80	2.7	174				
	Arg(NE)	80	3.0	173				
	Wat(O)	368	2.7					OP3 bridges the pyrophosphoryl group

^a The interactions observed in each structure are compared row by row. Hydrogen bonding is inferred if N–O or O–O distances are less than 3.4 Å and angles N–H–acceptor or C–O–acceptor are greater than 115° or 90°, respectively. The asterisk designates atoms in the ribityl moiety.

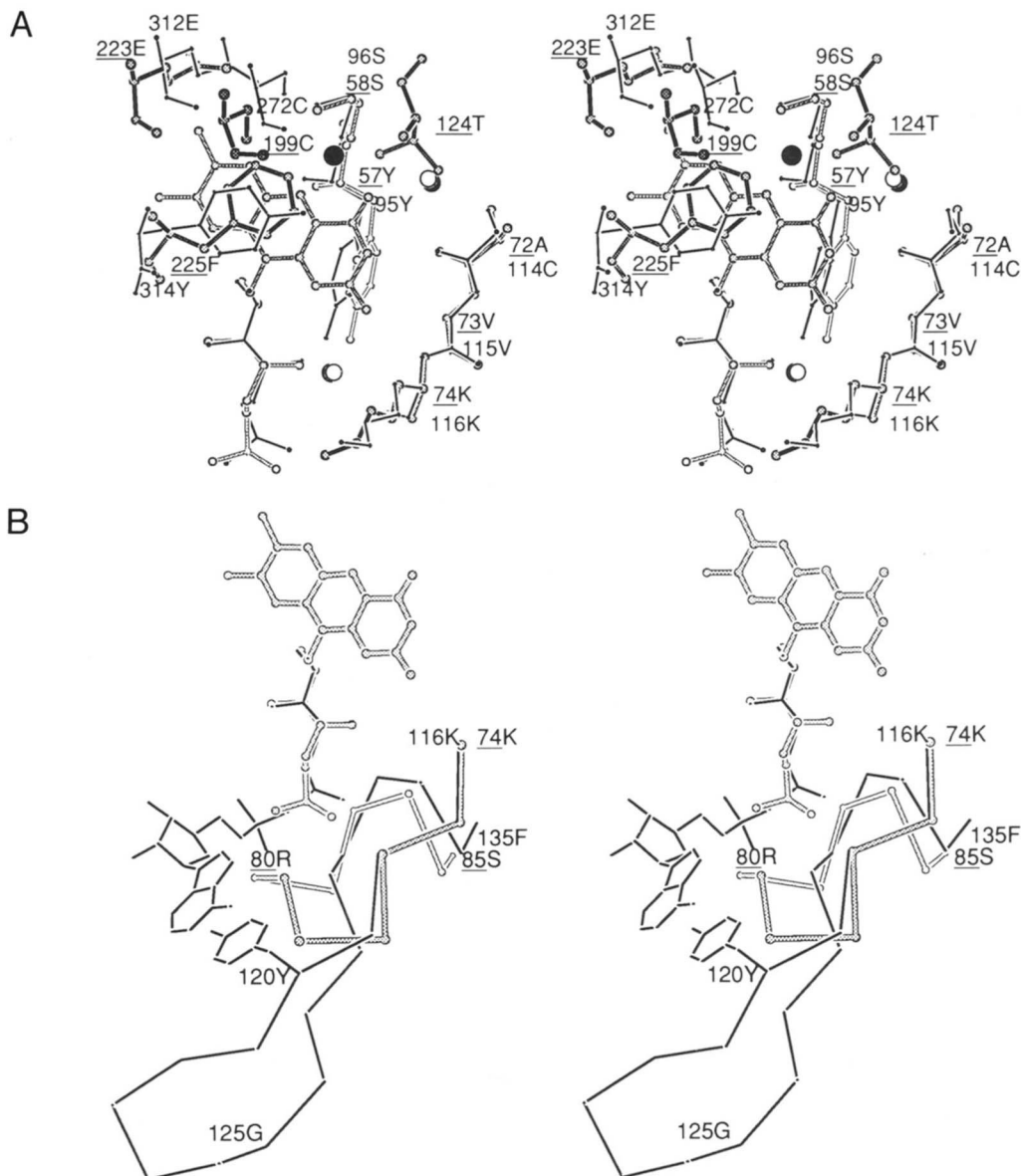


Fig. 6. Explanation on facing page.

FMN and FAD stems from the phosphate-binding site near the N-terminus of a short α -helix, around residues $^{79}\text{GRGGS}_{\text{PDR}}$ and $^{129}\text{KGVCS}_{\text{FNR}}$ (Fig. 6B,C). Gly 130_{FNR} is well conserved in homologous FAD-binding sequences (Andrews et al., 1992), but is replaced by arginine in the FMN-binding proteins PDR and vanB (Brunel & Davison, 1988). Glycine is required at this position in FNR to avoid steric interference with the distal phosphate of FAD and is thus an important determinant of selectivity between FMN and FAD. Arg 80_{PDR}, at the corresponding position, binds intimately to the FMN phosphate group, contributing further to specificity. However, because Arg 80_{PDR} is a surface residue, it may not be invariant in FMN-binding sites.

The sequence motif XGXX(S/T) is conserved in known family members that bind FAD. Only two homologues are known that bind FMN (PDR and vanillate demethylase), and these have the consensus XRGGS in the phosphate-binding region. A key distinction between the known proteins that bind FAD and those that bind FMN is the position of the conserved glycine, either two or three residues preceding the conserved Ser/Thr.

In FNR, residues from the β -hairpin at 119–129, which incorporates an eight-residue insert following 120_{FNR}, form part of the FAD-binding site (Fig. 6B). The hairpin residues make no hydrogen bonds with the adenine portion of FAD, but van der Waals contacts between the adenine ring and Tyr 120 can contribute to nucleotide-

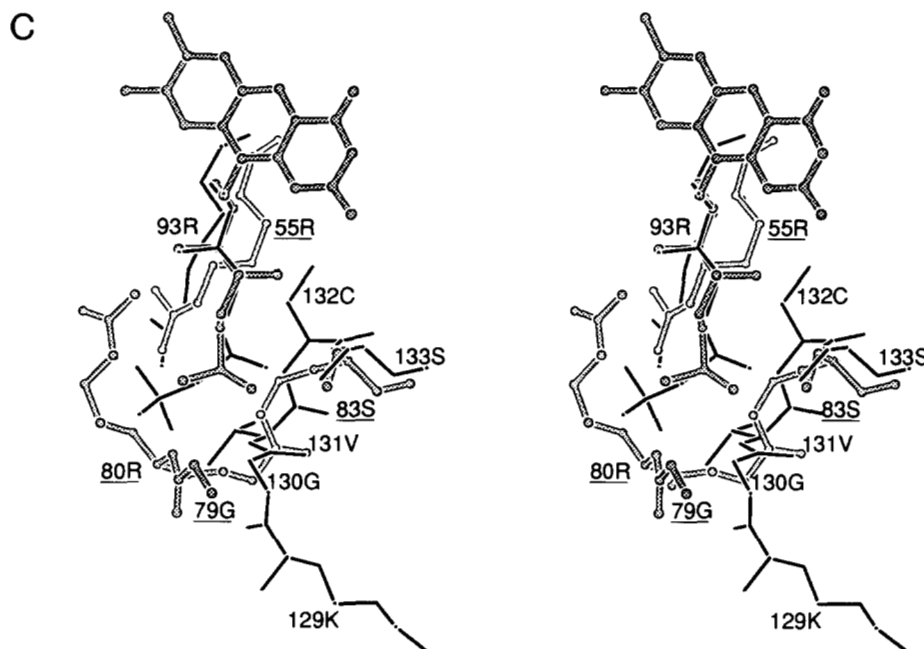


Fig. 6. (See also facing page.) Comparisons of the flavin-binding sites in FNR and PDR. Drawings of the region surrounding the flavin prosthetic group, with FNR bonds represented by thin bonds and PDR by thick bonds; PDR labels are underlined. Waters from PDR are represented as open circles and waters from FNR as filled circles. The riboflavin monophosphate atoms from PDR and FNR have been superimposed for these comparisons. For clarity, only one isoalloxazine ring has been drawn. Views are from the *re* side of the flavin ring. **A:** Interactions with the isoalloxazine rings. The fingerprint sequence that binds the flavin ring is RXYS (55–58_{PDR}, 93–96_{FNR}). Backbone interactions at 72–74_{PDR} or 114–116_{FNR} position the pyrimidine end of the ring. Flavin–protein hydrogen bonds involving these sequences are listed in Table 2. Residue substitutions in the vicinity of the flavin ring include Ala 72_{PDR} for Cys 114_{FNR}, Thr 124_{PDR} for Ala 175_{FNR}, and Phe 225_{PDR} for Tyr 314_{FNR}. A bound solvent (403) in FNR is hydrogen bonded to Tyr 314 and to O(4) and occupies a position similar to the side chain O γ of Thr 124_{PDR}. Residues Cys 199_{PDR} and Cys 272_{FNR} from the conserved sequence YXCG in the NAD(P) domains abut the aromatic rings stacked over the flavin and may contact bound nicotinamide. **B:** An overview of the flavin phosphate-binding sites, showing the β -hairpin insert of FNR. Residues 120–129 of FNR form a hairpin in which the initial Tyr stacks against the adenine ring of FAD; the adenine ribose OH groups interact with solvent. **C:** The binding sites for the ribityl chains and flavin phosphates. A view showing in detail the phosphate-binding sites of PDR and FNR, formed by the fingerprint sequences $^{79}\text{GRGGSPDR}$ and $^{129}\text{KGVCFSNR}$. Interactions of residues Arg 55, Gly 82, and Ser 83 with the flavin phosphate in PDR are similar in both proteins (see Table 2). The conserved serine residue forms hydrogen bonds to the proximal flavin phosphate in both PDR and FNR. Thus, this serine appears to contribute to phosphate binding but does not confer specificity for FMN versus FAD. However, the main chain preceding 130_{FNR} is displaced to allow the binding of the distal phosphate. Arg 80 of PDR has no match in FNR, and Gly residues have different conformations and positions in the $^{129}\text{KGVCFSNR}$ and $^{79}\text{GRGGSPDR}$ sequences. Gly 81_{PDR}, which initiates the helix, has unusual dihedral angles (113° , -15°), whereas Gly 82_{PDR} does not have a special conformation.

binding selectivity. It should be noted that residue insertions in this segment are not a sure indicator of flavin nucleotide specificity. In at least one FAD-binding protein (methane monooxygenase component C), the spacing between the consensus sequences RXYS and GXXS (Stainthorpe et al., 1990) is similar to that in PDR.

Pyridine nucleotide binding and specificity in FNR and PDR

Binding sites for adenosine phosphates

Selective recognition of NADP⁺ (vs. NAD⁺) by FNR involves interactions near the adenylate 2'-phosphate, and

is determined partly by the fourth fingerprint sequence, starting near the C-terminus of the N β 3 strand at residue 233_{FNR}. The features involved in selectivity for 2'-phospho AMP versus AMP are illustrated in Figure 7A and B, which depict the complexes of FNR with 2'-phospho AMP and PDR with NADH. Residues Ser 234, Arg 235, and Tyr 246 of FNR hydrogen bond directly to the 2'-phosphate, and Lys 244 may also interact weakly with the phosphate. In PDR, Asp 173 replaces Ser 234_{FNR} and forms a hydrogen bond with the 2'OH group, contributing to nucleotide specificity (Fig. 7B; Kinemage 5). An acidic side chain with this function is a hallmark of many NAD⁺-binding proteins (Wierenga et al., 1986).

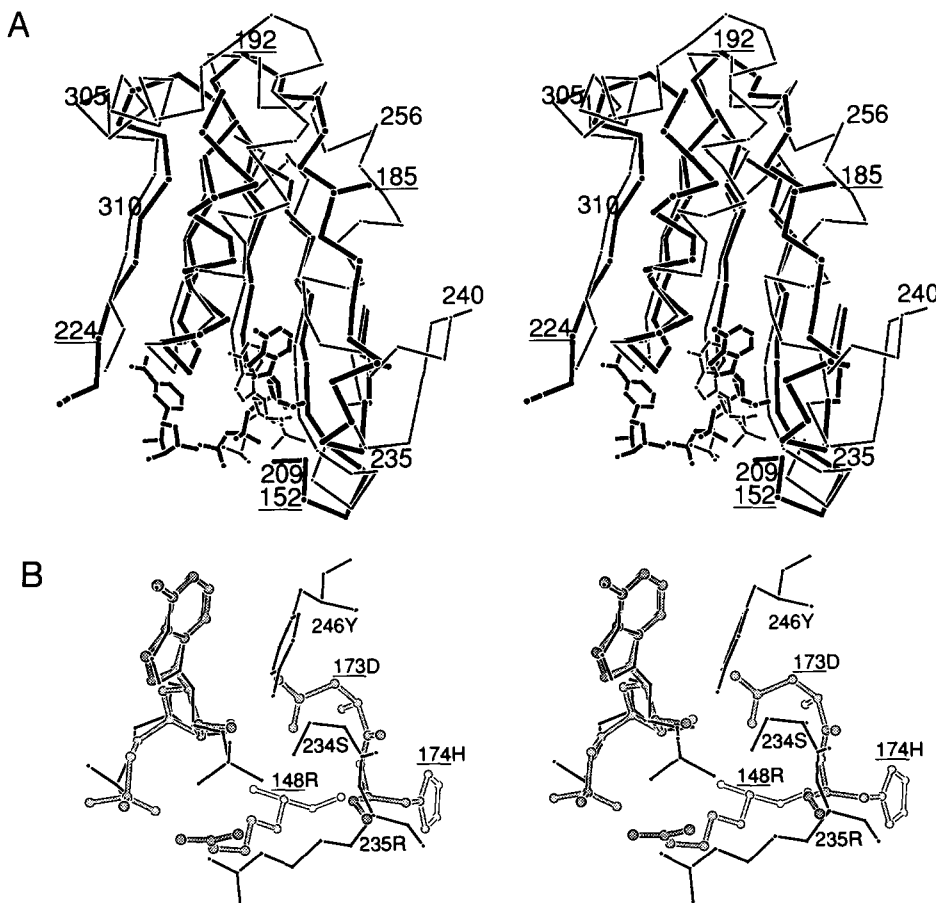


Fig. 7. Explanation on facing page.

At His 174_{PDR}, which replaces Arg 235_{FNR}, the main chain of PDR turns sharply from the path taken by FNR. The shape of the region that binds the adenylate group is altered in FNR, relative to PDR, by folding out of the loop beyond residue 235 and the intrusion of helix Nα3'.

Pyridine nucleotide specificity has been examined in the glutathione reductase family, both by mutation and by comparison of glutathione reductase with lipoamide dehydrogenase. Several of the residues implicated in the selectivity for NADP⁺ versus NAD⁺ in FNR and PDR have counterparts in the glutathione reductase family of flavoproteins. Mutation of residues functionally analogous to Arg 235_{FNR} and Asp 173_{PDR} has been shown to alter pyridine nucleotide selectivity in glutathione reductase. While mutations at a single site in GR have a major effect, full conversion to selectivity for NAD⁺ requires many residue interchanges (Scrutton et al., 1990). Comparisons of NADP⁺-specific GR with the closely related NAD⁺-specific lipoamide dehydrogenase reveal several differences in the pyridine nucleotide sites, with local backbone changes in the vicinity of the acidic residue, Glu 201, which interacts with the adenine ribose (Mattevi et al., 1992; Bocanegra et al., 1993). Overlay of the FNR

and PDR structures shows that changes in pyridine nucleotide selectivity may be accompanied by alterations in the backbone that are more extensive than those found by comparison of GR and lipoamide dehydrogenase.

Binding sites for pyridine nucleotide phosphates

The adenosine 5'-phosphate groups of NAD(H) or 2'-phospho AMP bind near the initial glycine of the finger-print sequence GXGXXP (120–125_{PDR} or 171–176_{FNR}). We assume that the sites occupied by the AMP moieties in the observed complexes (Fig. 7A) are also characteristic for intermediates in hydride transfer. In both PDR and FNR, the local conformation is characterized by phi, psi of (60°, -130°) and (-60°, 0°) at the two glycine residues, the first of which occupies position 2 of a type II' turn. As can be seen in Figure 7C, the II' turn determines the position of the bound pyridine nucleotide diphosphate. The first glycine of the sequence GXGXXP is required not only because of its unusual conformation but also to allow the diphosphate to approach the backbone of the turn. The second glycine may be required to avoid steric overlap with bound nicotinamide or with the Sγ atom of the well-conserved cysteine in segment 5 of Figure 1.

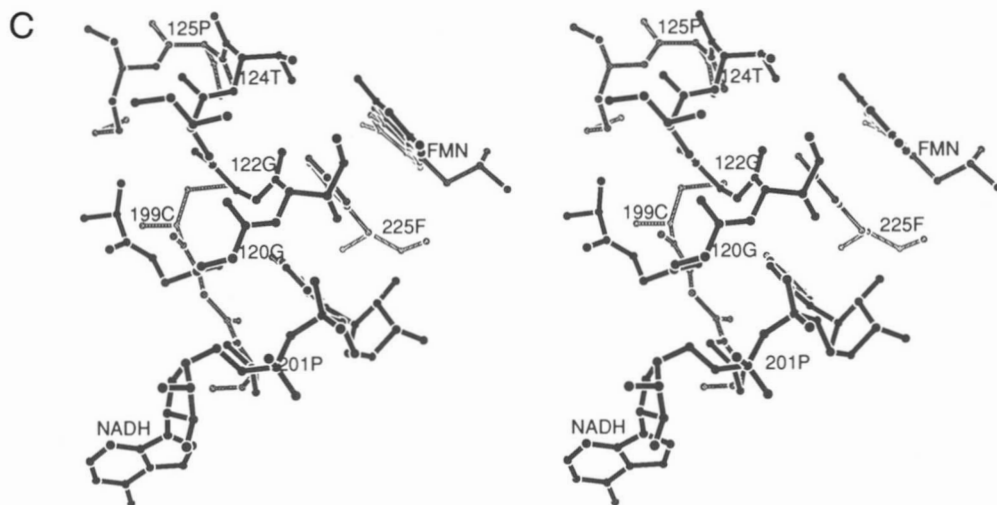


Fig. 7. (See also facing page.) The pyridine nucleotide-binding sites in FNR and PDR. **A:** Backbones of the oxidized forms of PDR and FNR in the vicinity of the pyridine nucleotide-binding sites. The superposition was determined by the same least-squares fitting of backbone atoms used in Figure 2A. The complex of FNR with 2'-phospho AMP is drawn with thin bonds and PDR²⁻:NADH is drawn with thick bonds and underlined residue labels. Insertions and variations in the main chain, as well as residue substitutions, affect the shape of the adenosine binding region. The bound nucleoside is positioned somewhat differently in PDR and FNR. The loop and the helix Nα3, formed by residues 235–255 of FNR, have no equivalents in PDR. This view also shows the extra Nα4' helix of FNR, which precedes residue 305, and follows the elongated helix Nα4. The side chain interactions that are important in conferring specificity for NADP⁺ versus NAD⁺ are shown in panel B. **B:** A detailed comparison of the adenosine-binding subsites in FNR and PDR. In contrast to panel A, the alignment was determined by local matching of the adenosine groups. Underlined numbers and thick bonds designate residues from PDR. Coordinates are from the ligated species (see Methods). Residues Ser 234_{FNR}, Arg 235_{FNR}, and Tyr 246_{FNR} make the principal contacts with the 2'-phosphate in FNR, whereas Asp 173_{PDR} is hydrogen bonded to the adenine ribose hydroxyls in the PDR complex. In the ligated NAD⁺-specific PDR, the guanidinium moiety of Arg 148 occupies approximately the same position as Arg 235_{FNR}, but their positions in the sequence and their roles in binding are different. Arg 148_{PDR} interacts with the 5'-phosphate and Arg 235_{FNR} with the 2' phosphate. **C:** The interactions between bound NADH and the fingerprint turn in PDR. The orientation of bound nicotinamide is from the observed PDR²⁻:NADH complex (Correll, 1992; Correll et al., 1992). Hydride transfer is expected to require displacement of Phe 225 by nicotinamide (see text); the nicotinamide site in the PDR²⁻:NADH complex shown here represents an alternative binding mode. Close approach of the adenosine 5' phosphate to position 120 requires that this residue be Gly. NH 121 is hydrogen bonded to the oxygen of the nicotinamide phosphate in this observed PDR²⁻:NADH complex, but we cannot assign with certainty the position of the nicotinamide phosphate in the intermediates formed during hydride transfer. The conserved Pro 125, at the start of helix Nα1, is close to the ring of the conserved Phe 225, which is presumably replaced by the nicotinamide ring during hydride transfer. Part of the fifth fingerprint sequence, including the conserved CG, is seen at the back, with the sulfur of Cys 199 close to Phe 225. This contact is shown in another perspective in Figure 6A.

Strong conservation of the sequence GXGXXP suggests that the conformation and function of this turn are also conserved among family members. The conserved proline (Segal et al., 1992) probably contacts bound nicotinamide (see below).

Binding sites for nicotinamide

The reaction with pyridine nucleotides is expected to proceed by hydride transfer, utilizing an intermediate in which the nicotinamide ring is stacked or in contact with isoalloxazine, as observed in the complex of reduced glutathione reductase with NADPH (Pai et al., 1988; Karplus & Schulz, 1989). This expectation is based on observations from kinetic studies. Consistent with hydride transfer, a kinetic isotope effect of at least 6.0 has been determined for reduction of PDR by NADD (Ballou et al., in press). In addition, the transient intermediates in reduction of

PDR (Batie & Ballou, 1987) and FNR (Massey et al., 1970; Batie & Kamin, 1986) display charge transfer spectra characteristic of flavin-nicotinamide stacking (Massey & Ghisla, 1974).

In the absence of X-ray data for a complex that mimics the expected intermediate, the orientation of bound nicotinamide has been inferred from models (Karplus, 1991; Correll, 1992). The nicotinamide ring in the postulated pyridine nucleotide complex of PDR replaces the side chain of Phe 225, and the AMP moiety occupies the site observed in a series of pyridine nucleotide complexes of FNR and PDR (see above). In the model PDR:NADH complex, Pro from the sequence ¹²⁰GIGITP_{PDR} and Cys from ¹⁹⁹CG_{PDR} (Fig. 1) contact the bound nicotinamide. The analogous contacts of Phe 225_{PDR} with Pro 125_{PDR} and Cys 199_{PDR} are shown in Figures 6A and 7C. The consequences of mutation furnish complementary evi-

dence that cysteine in the conserved sequence CG is associated with pyridine nucleotide binding. The Cys 272 Ser mutant of FNR displays decreased rates of flavin reduction by NADPH and lower yields of intermediate pyridine nucleotide:flavin charge transfer species (Aliverti et al., 1993). The glycine of the conserved CG in this fingerprint sequence is at the end of a parallel sheet strand, but it adopts somewhat unusual conformations in FNR ($\phi = 141^\circ$, $\psi = -148^\circ$) and in PDR ($\phi = -179^\circ$, $\psi = -171^\circ$). The precise roles of the CG sequence remain to be established.

Some comparisons with glutathione reductase and other flavoproteins

The FNR and GR families of flavoproteins both react with pyridine nucleotides, and each family incorporates separate domains that recognize flavin and pyridine nucleotides. Although the domains that bind pyridine nucleotides are both based on a parallel β -sheet of similar topology, the domains that bind flavin nucleotides differ markedly. The antiparallel barrel topology in the flavin domain of FNR is unrelated to the α/β parallel sheet fold found in GR and its relatives. Furthermore, each of the domains in PDR and FNR is formed from contiguous sequences, whereas the flavin domain in GR is a more complex structure formed from noncontiguous segments of the polypeptide sequence. The fingerprints for the flavin-binding domain of human GR are a phosphate-binding sequence $^{27}\text{G}X\text{GXXG}$ in a β -loop- α motif near the N-terminus, an acidic residue at 50 in a following β -strand, and a sequence far downstream (321–331) in the final strand of the parallel sheet, which interacts with the ribityl group (Eggink et al., 1990; Schulz, 1992). In contrast, the sequences responsible for mono- or diphosphate binding in the FNR family occur 25–35 residues downstream from those that interact with the isoalloxazine ring (Andrews et al., 1992). In view of the dissimilarities in flavin-binding folds, it is not surprising that the local sequences that bind the flavin phosphates in PDR and FNR form structures that are distinct from the flavin phosphate site in GR (Fig. 8).

Flavin phosphates are bound to β -connector- α motifs in many flavoproteins (Mathews, 1991), but the connector sequences and conformations exhibit considerable diversity. Several variants of the connector sequences and structures have been observed. One group of phosphate sites (Eggink et al., 1990; Schulz, 1992) conforms to the dinucleotide-binding sequence pattern GXGXXG , which is found to bind flavin phosphates in the GR family. FMN phosphate sites in flavodoxins (Ludwig & Luschinsky, 1992) have a different motif, SGTGXT, forming a tight loop in which backbone NH and conserved Ser or Thr side chains hydrogen bond to phosphate oxygens. Some

of the interactions in PDR resemble those in flavodoxin (Fig. 8B). In glycolate oxidase the FMN phosphate interacts with the start of a helix and with two parallel β -strands; the latter are connected by an intervening 20-residue segment of the α/β -barrel domain (Lindqvist, 1989). In contrast, the β -strand residues that bind the FAD phosphate in FNR are part of an antiparallel hairpin. The phosphate-binding loop of PDR differs from FNR (Fig. 6C) and from the β -loop- α sites in other flavoproteins (Fig. 8B).

Local differences in the region that binds the pyridine nucleotide phosphates distinguish the FNR family from the GR family (Karplus et al., 1991). As can be seen from Figure 9, the phosphate-binding sequence in the NAD^+ domain of PDR (or the NADP^+ domain of FNR) forms a tight II' turn rather than the more open loop found in GR and in the classic dinucleotide-binding fold (Wierenga et al., 1986). The bound adenosine phosphates do not superimpose when the β -loop- α motifs of PDR and GR are aligned.

Redox potentials of the flavins in PDR and FNR

The two-electron midpoint potential ($E'_\text{ox/red}$) for the flavin in PDR is -230 mV (Batie et al., in prep.), whereas in FNR the corresponding potential is about -350 mV (Keirns & Wang, 1972; Batie & Kamin, 1981). In both proteins, reduction to the semiquinone form entails addition of one electron and one proton to yield a species with absorbance near 580 nm and protonated at N(5) (Batie & Kamin, 1981, 1984; Batie & Ballou, 1987). The fully reduced species are formed by the further addition of one electron to yield an anionic flavin. The redox properties of these protein-bound flavin species depend on selective hydrogen bonding to ring atoms N(1), O(2), O(4), and N(5). Stabilization of the anionic reduced flavin, which will raise the redox potential for the ox/red equilibrium, requires compensation of the net negative charge, which is delocalized with significant negative density on atoms N(1), O(2), O(4), and C(4a) (Hall et al., 1987a,b). Examination of the isoalloxazine-protein interactions in FNR and PDR reveals several differences, each of which may contribute to easier reduction of the flavin in PDR.

The most obvious variations in the isoalloxazine environments of oxidized FNR and PDR occur in the vicinity of the O(4) and N(5) flavin atoms and are associated with the substitutions of $\text{Thr 124}_{\text{PDR}}$ for $\text{Ala 175}_{\text{FNR}}$ and $\text{Phe 225}_{\text{PDR}}$ for $\text{Tyr 314}_{\text{FNR}}$ (Fig. 6A; Table 2). In FNR, a solvent is hydrogen bonded to Tyr 314, to the backbone oxygen of Thr 172, and to O(4). In PDR, this bridging solvent is lost and the solvent:O(4) interaction is replaced by a hydrogen bond between the side chain of $\text{Thr 124}_{\text{PDR}}$ and FMN O(4). Replacing a stacked Tyr by Phe in *D. vulgaris* flavodoxin increases the $2e^-$ midpoint potential, but

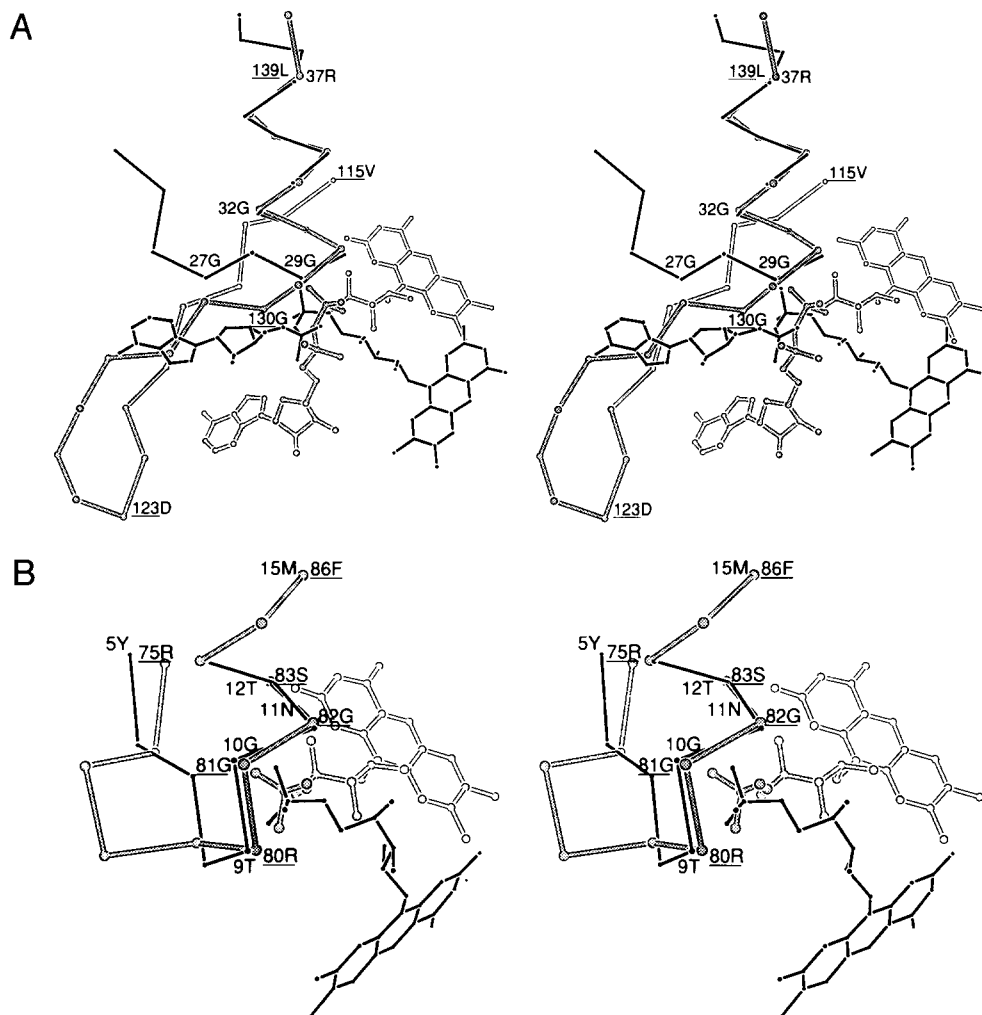


Fig. 8. Flavin phosphate-binding sites in FNR and glutathione reductase, and in flavodoxin and PDR. A common theme in all these structures is a β -connector- α motif, but each of the sites is distinguished by different sequence patterns and structural patterns. Alignments are based on the helices, and include the glycines that occur at the helix starts. **A:** Comparison of flavin phosphate sites in FNR and GR, with FNR designated by thick bonds and underlined residue labels. **B:** Comparison of sites in flavodoxin (Ludwig & Luschinsky, 1992) and PDR, with PDR designated by thick bonds and underlined labels.

by only 14 mV (Swenson et al., 1991). The exchange of aromatics may have more significant effects in the FNR family.

Comparisons of the refined structures of oxidized FNR and PDR (Table 2) show small differences in the interactions of Ser 58_{PDR} and Ser 96_{FNR} with the O(4) and N(5) flavin atoms. The variations in observed distances and angles are of the order of 0.2–0.3 Å and 20° (Table 2), at the limit of significance even for these refined structures, but are all consistent with stronger hydrogen bonding between Ser 96_{FNR} NH and N(5) in oxidized FNR and stronger bonding between Ser 58_{PDR} NH and O(4) in PDR. These differences would lower the potential of FNR relative to PDR by stabilizing the oxidized state in FNR and the reduced state in PDR. Preliminary analyses of the

fully reduced proteins indicate similar consequences of two-electron reduction in both proteins: the formation of a hydrogen bond between NH(5) and O γ of Ser 58_{PDR} or Ser 96_{FNR} in the reduced state, and association of a solvent at N(1). The absence of more dramatic structural differences in the flavin-binding sites of PDR and FNR is surprising, given the magnitude of the redox potential difference.

Redox potentials of [2Fe-2S] in PDR and ferredoxin

High [2Fe-2S] potentials, above –200 mV, are characteristic of dioxygenase reductases like PDR. The [2Fe-2S]

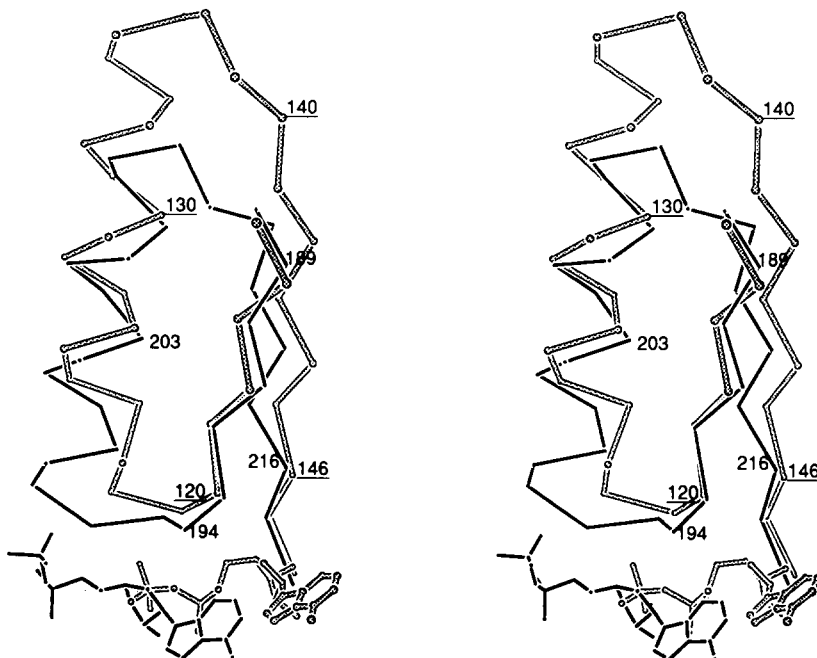


Fig. 9. A local comparison of the pyridine nucleotide domains of PDR and glutathione reductase. The drawing shows the position and orientation of the fingerprint phosphate-binding loops that distinguish the pyridine nucleotide sites of the GR and FNR families of proteins, along with the ADP moieties of the nucleotide ligands. PDR residues (thick bonds) are designated with underlined labels. The backbones of the β - α - β motif in the pyridine nucleotide domains are aligned to overlay the Gly residues (120_{PDR} and 194_{GR}) that are characteristic determinants of each structure. The conformations are ($\phi, \psi = 140^\circ, 165^\circ$) at Gly 194 of GR and ($\phi, \psi = 60^\circ, -130^\circ$) at Gly 120 of PDR.

center in PDR has the relatively high potential¹ of -174 mV, whereas the [2Fe-2S] sites in plant ferredoxins are reduced² at potentials of -240 to -460 mV (Cammack, 1992). Using comparisons with *Anabaena* 7120 ferredoxin, which is reduced at a potential of about -440 mV (Hurley et al., 1993), we have looked for structural features that may contribute to the unusually high potential of the [2Fe-2S] center in PDR. The structure of the ferredoxin from *Anabaena* 7120 (Rypniewski et al., 1991) was selected for detailed comparison because it had been refined at 1.7 Å resolution (H.M. Holden, pers. comm.).

The redox potentials exhibited by iron-sulfur clusters can be modulated by $\text{NH} \cdots \text{S}$ hydrogen bonds (Carter et al., 1972), by nonbonded contacts with aromatic residues (Markley et al., 1986), and by ligand substitution (Gurbel et al., 1989; Werth et al., 1990). Although hydrogen bonding has been the focus of many discussions of potentials in iron-sulfur proteins (Carter, 1977), recent studies of HiPIPs and [4Fe-4S] ferredoxins (Backes et al., 1991; Rayment et al., 1992) verify that protein:cluster hydrogen bonding is conserved within the HiPIP or ferredoxin classes of [4Fe-4S] proteins despite considerable

variations in redox potentials. Other parameters such as distance from the solvent boundary and the polarity of the cluster environment must also have significant effects on the redox potentials of these [4Fe-4S] proteins. Our observations and calculations on PDR and *Anabaena* Fd, reported below, show that variation in hydrogen bonding is a major device for modulation of redox potentials of structurally similar [2Fe-2S] proteins.

*The [2Fe-2S] environments in *Anabaena* ferredoxin and PDR*

Superposition of the PDR and *Anabaena* Fd structures reveals differences in the details of the interactions between the $\text{Fe}_2\text{S}_2\text{Cys}_4$ cluster and these proteins. Hydrogen bonding of the S^{2-} cluster atoms and cysteine sulfurs is compared in Table 3. According to the criteria adopted in that table, there are three more NH or OH donors to sulfur in PDR than in *Anabaena* Fd. These net differences in hydrogen bonding should increase the redox potential of PDR relative to Fd.

Local alignment of the cluster atoms and ligands reveals a significant difference in the backbone conformations of the 46-47_{Fd} peptide and its equivalent, 277-278_{PDR} (Fig. 10). In Fd, the oxygen of the C-O dipole is only 3.2 Å from the S^{2-} atom denoted S2, whereas in PDR the peptide group is rotated by ca. 180° so that the amide NH 278 points toward this S^{2-} atom (Fig. 10). Some of the differential hydrogen bonding is a consequence of the change in orientation of this peptide (Table 3): two strong $\text{NH} \cdots \text{S}$ interactions that have no equivalents in Fd are formed by NH 277 and NH 278 in PDR, and the alternative orientation in Fd leads to a single strong $\text{NH} \cdots \text{S}$ interaction at NH 46_{Fd}. The importance of the

¹ Adrenodoxin and putidaredoxin also have higher potentials than most plant ferredoxins, at -250 and -240 mV, respectively (Sligar & Gunsalus, 1976; Huang et al., 1983). Unlike PDR, they possess Cys loop sequences with a pattern different from plant Fds, and their epr spectra display axial rather than rhombic symmetry.

² When the [2Fe-2S] cluster in ferredoxins is reduced, the added electron is predominantly localized on one Fe (Dunham et al., 1971; Poe et al., 1971; Salmeen & Palmer, 1972). Recent NMR studies of plant Fds (Dugad et al., 1990; Skjeldal et al., 1991) have established that Fe1, the iron nearest the surface, is reduced. See Noddleman et al. (1985) and Noddleman and Case (1992) for molecular orbital calculations on [2Fe-2S] species.

Table 3. Protein:[2Fe-2S] interactions in PDR and *Anabaena* Fd^a

Interactions in PDR				Interactions in <i>Anabaena</i> Fd			
Source atom	Target atom	Distance (Å)	Angle (degrees)	Source atom	Target atom	Distance (Å)	Angle (degrees)
SG Cys 272	N Ser 274	3.4	163	SG Cys 41	N Ala 43	3.1	158
	N Thr 276	3.4	162		N Ala 45	3.4	150
	OG1 Thr 276	3.5	122		No equivalent: 45 is Ala		
	N Cys 277 ^b	3.3	150		N Cys 46	3.8	91
	N Gly 275 ^b	3.5	121		N Gly 44	3.7	104
SG Cys 277	OG Ser 279	3.3	93	SG Cys 46	OG1 Thr 48	3.4	93
	OG Ser 271	3.2	129		OG Ser 40	4.7	54
	N Ser 279	3.5	164		N Thr 48	3.4	154
SG Cys 280	N Cys 308	3.5	156	SG Cys 49	N Cys 79	3.4	169
SG Cys 308	N Gly 275 ^b	3.5	117	SG Cys 79	N Gly 44	3.6	142
S1 FeS 323	N Glu 273	3.5	157	S1 FeS 100	N Arg 42	3.2	159
	N Ser 271	3.6	150		N Ser 40	3.4	171
S2 FeS 323	N Gly 278	3.4	150	S2 FeS 100	N Ser 47	4.7	44
	N Cys 277 ^b	3.6	130		N Cys 46	3.3	151

^a Hydrogen bonds to sulfurs of the Fe₂S₂Cys₄ clusters in PDR and *Anabaena* Fd are compared. Hydrogen bonding is inferred if N-S or O-S distances are less than or equal to 3.7 Å and angles N-H-S or C-O-S are greater than 115° or 90°, respectively. Interactions that do not meet these criteria are italicized. In PDR, Gly 275 NH and Cys 277 NH each interact with two acceptors; the corresponding NH groups in Fd select one or the other acceptor.

^b Donor to two sulfurs.

orientation of the peptide 277–278_{PDR} is borne out by calculations of electrostatic interactions, described below.

The presence of Gly at position 278, following the second Cys ligand to Fe1, may determine the choice of peptide orientation and the patterns of NH···S hydrogen bonding. Gly 278 in PDR adopts a conformation ($\phi = 84^\circ$, $\psi = -4^\circ$) that is disallowed for other residues. The corresponding residue is Ser or Thr in plant Fd sequences (Matsubara & Hase, 1983; NBRF Database), except for *Halobacterium halobium* Fd, where it is Ala. The peptide

at the equivalent Ser 47 in *Anabaena* Fd assumes a conformation ($\phi = -116^\circ$, $\psi = 0^\circ$) close to the normal β region, as do the corresponding peptides in the structures of *S. platensis* (Fukuyama et al., 1980), *Aphanothecce sacrum* (Tsukihara et al., 1987), and *H. halobium* (Sussman et al., 1986; Sussman, pers. comm.) ferredoxins. Among the reductases related to PDR, Gly follows the second Cys ligand in vanillate demethylase reductase (Brunel & Davison, 1988), benzoate dioxygenase reductase (Neidle et al., 1991), and xylene monooxygenase reductase (Suzuki et al.,

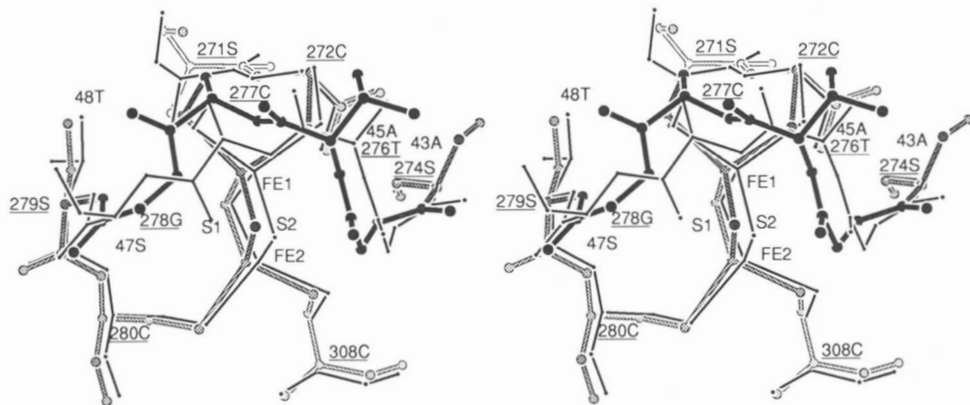


Fig. 10. A superposition of the [2Fe-2S] clusters and surrounding residues in PDR and *Anabaena* Fd. For this comparison the iron-sulfur loops were aligned using the [2Fe-2S] cluster atoms and three cysteine ligands (41, 49, and 79 of Fd). *Anabaena* Fd bonds are drawn with thinner lines; PDR atom labels are underlined. Differences in the orientation of the peptide following the second Cys ligand to Fe1 (277–278 in PDR) can be seen in the upper left area of the drawing, along with the interaction NH46-S2 in Fd. The PDR and Fd backbone conformations are similar at the remaining residues of the [2Fe-2S]-binding loop, but the side chains differ at positions 40 and 45 of Fd. See Table 3.

1991). An exception is methane monooxygenase component C, with Ala at the equivalent position (Stainthorpe et al., 1990) and a [2Fe–2S] potential of –220 mV (Lund & Dalton, 1985).

Electrostatics calculations

To estimate the relative contributions of charge distribution, hydrogen bonding, and other dipole interactions to modulation of the redox potentials, we calculated the magnitudes of the electrostatic interactions between the protein and the cluster atoms (see Methods). The approach was the same as used by Gilson and Honig (1988a) and by Soman et al. (1989) in studies of *pK* shifts induced by electrostatic interactions. Assuming additivity of the electrostatic potentials (Sharp & Honig, 1990), one can estimate the contributions of specific charges, such as the partial charges representing peptide dipoles, by comparing the interaction energies when these charges are included with the energies when they are omitted. The results are presented in Table 4.

The starting point was the calculation of the electrostatic potentials generated at the cluster atoms by all of the other charges, using only the atoms of the third domain of PDR. The computed electrostatic potentials were found to be uniformly higher in PDR than in Fd, indicating that addition of an electron to the iron-sulfur center of PDR is energetically more favorable than addition of an electron to Fd. Differences in the electrostatic interaction energies calculated for PDR and Fd are reported in the first line of Table 4.

Interactions between the Fe₂S₂Cys₄ atoms and charged groups (side chains and terminal residues) were computed by setting to zero the partial charges on all neutral peptide and side-chain dipoles, leaving only formal point

charges at the ionized side chains and chain termini (Table 4, line 2). The differences between the energies shown in lines 1 and 2 are a measure of the contribution of the dipoles (partial charges) in each protein. Despite the large difference between the net charges of Fd and the third domain of PDR (–16 for oxidized Fd and –3 for the [2Fe–2S] domain of oxidized PDR), the calculated electrostatic interactions between the iron-sulfur cluster and the charged groups are very similar in the two proteins (Table 4, line 2). The charged acidic or basic side chains are not very close to the [2Fe–2S] cluster atoms in either protein: in PDR the nearest formal charges are at Glu 273 and Arg 262, 5.9 and 7.5 Å away, and are partly exposed to solvent. A similar insensitivity to surface charge was observed in experiments and calculations on electrostatic effects in trypsin (Soman et al., 1989) and in calculations on [4Fe–4S] proteins by Langen et al. (1992).

The dipole interactions that make the major contributions to the higher electrostatic potentials at Fe₂S₂Cys₄ in PDR depend strongly on dipole distance and orientation. The contributions of the nine peptides closest to the cluster, 271–279 and 308_{PDR} or 40–48 and 79_{Fd}, account for about 60% of the difference in electrostatic interaction energy that distinguishes PDR from Fd (Table 4, line 3). The peptides at 46–47_{Fd} or 277–278_{PDR} dominate the differences because of their opposite orientations (Fig. 10). Omitting the charges on the backbone atoms in Cys 46 and the N, H, and C α of Ser 47 hardly changes the electrostatic interaction energy in Fd, but omitting the charges on the comparable atoms in PDR decreases the favorable electrostatic interaction by approximately 2 kcal/mol (Table 4, line 4).

Calculated interactions of the polar side chains, in particular the threonine and serine side chains in the iron-binding sequences, are reported in lines 5 and 6 of Table 4. Positions of the O and H atoms of Thr and Ser are not

Table 4. Changes in electrostatic interaction energies accompanying reduction of the iron-sulfur clusters in PDR and Fd^a

Assigned charges	PDR (kcal/mol)	Fd (kcal/mol)	Difference (PDR – Fd)		Contribution of omitted charges
			kcal/mol	mV	
1. Formal charges and dipoles	–22.31	–17.07	–5.24	227	
2. Omitting all dipoles	1.82	1.97	–0.15	7	97%
3. Omitting nine peptide dipoles	–8.26	–6.28	–1.98	86	62%
4. Omitting 277/278 or 46/47 peptide	–20.06	–17.31	–2.74	119	48%
5. Omitting Ser/Thr OH at cluster	–20.00	–15.77	–4.23	183	19%
6. Omitting all side chain dipoles	–19.16	–16.13	–3.03	132	42%

^a Energies were computed by summing over the potentials at each of the cluster atoms, as described in Methods. The energies in line 1 are negative, favoring reduction, because the electrostatic potentials generated at the cluster atoms were all positive. The “Difference” columns compare the interactions in PDR and Fd on kcal/mol and mV scales. The calculations reported here are for the excised third domain of PDR. Potentials were computed at a scale of 1.13 grid units/Å for both proteins. Dipole contributions of the same magnitude as in line 2 are also obtained from a calculation that sets all the formal charges to 0.0.

as accurate as those of backbone atoms, but calculations with the refined coordinates suggest that variations in the Ser and Thr interactions with the cluster contribute about 1.0 kcal/mol to the differences between Fd and PDR. Comparison of contributions from all neutral polar side chains, including the serine and threonine residues in contact with the Fe₂S₂Cys₄ cluster (Table 4, line 6), with the contributions of serine and threonine at the cluster (Table 4, line 5) provides evidence for some modulation of the redox potentials by side chains not in contact with the iron-sulfur center.

The electrostatic interaction energies are not the only factors determining free energies for reduction of the clusters. A complete calculation of redox potentials must include the solvation energies of the clusters in each protein and appropriate scaling to model compounds. In computations of the potentials of reaction center hemes, Gunner and Honig (1991) determined relative solvation energies (Gilson & Honig, 1988b) with magnitudes that ranged from 30 to 60% of the calculated electrostatic interactions between the hemes and the protein. Computations on [4Fe-4S] proteins using the microscopic electrostatic model developed by Warshel and coworkers (Langen et al., 1992) demonstrate similar effects of solvent interactions. The approximate correspondence of the computed differences in electrostatic interactions with measured potential differences between Fd and PDR (Table 4) may arise because solvation energies are very similar for the [2Fe-2S] clusters in the closely related Fd and PDR folds.

As expected, the calculations verify that differences in the strength and number of hydrogen bonds have important effects on the electrostatic interactions between the protein and the [2Fe-2S] cluster. The computations also show that surface charges have relatively small effects and support the idea that polar groups not in contact with the cluster can alter redox potentials (Backes et al., 1991).

Conclusion

We are fortunate to have as the first examples of structures in the FNR family two proteins that are so different. One is prokaryotic and the other eukaryotic. They share only 15% sequence identity and differ with respect to prosthetic groups, substrates, directions of electron transfer, and association with one-electron carriers. Yet their overall folds are nearly identical. The comparison of PDR with FNR provides another striking demonstration of the power of three-dimensional structures as tools in ascertaining evolutionary relationships. The functional differentiation of these two proteins depends on relatively small variations in the structures of the flavin, pyridine nucleotide, and [2Fe-2S]-binding sites. These differences nevertheless have profound effects on the energetics of the oxidation-reduction reactions.

Methods

Structure determinations

Analyses of FNR and PDR

The structure analysis of ferredoxin-NADP⁺-reductase has been described (Karplus et al., 1991), and the coordinates deposited in the Protein Data Bank as 1FNR for the oxidized structure and 2FNR for the 2'-phospho AMP complex. Subsequent refinement (Tronrud et al., 1987) of the structure has decreased *R* to 0.190 for all data (37,621 reflections) between 10.0 and 1.7 Å for the native structure and to 0.185 (36,903 reflections) for FNR bound to 2'-phospho AMP (Bruns & Karplus, in prep.). Comparisons in this paper are based on the refined coordinates. The structure of oxidized phthalate dioxygenase reductase (Correll et al., 1992) has been refined to an *R* of 0.186 for all data (23,710 reflections) from 10.0 to 2.0 Å and coordinates deposited in the Protein Data Bank (2PIA). The orientation of the backbone surrounding the [2Fe-2S] cluster in oxidized PDR was verified in maps computed after omit-refinement (Brünger et al., 1990; Brünger, 1992). The structure of PDR²⁻ bound to NADH has been refined to an *R* of 0.185 for all data (23,784 reflections) from 10.0 to 2.0 Å, and the structure of the fully reduced form, PDR³⁻, to an *R* of 0.185 for all data (23,083 reflections) from 10.0 to 2.0 Å.

Binding sites for pyridine nucleotides were identified by analysis of crystals soaked in nucleotides, nucleotide fragments, or nucleotide analogs. In the case of FNR, the primary information about pyridine nucleotide interactions is derived from a complex with 2'-phospho AMP. With PDR, binding sites have been observed for both the adenine nucleotide and nicotinamide nucleotide moieties. The nicotinamide portion is visible only when NADH is bound to partly reduced crystals (Correll et al., 1992). Epr spectra of these crystals are consistent with the assignment of the oxidation state of the protein in the crystalline complex as predominantly the two-electron reduced species, PDR²⁻ (W.R. Dunham, pers. comm.).

Structure analysis of *Anabaena* 7120 ferredoxin

A structure of the oxidized form, based on data to 2.5 Å, has been described (Rypniewski et al., 1991). Subsequently, the refinement has been continued with data to 1.7 Å resolution (H.M. Holden, pers. comm.). Coordinates for the high-resolution structure were used in the comparisons and computations.

Alignments of structures and sequences

Initial superposition of structures was performed interactively on a computer graphics workstation with the program TOM (Cambillau & Horjales, 1987) to determine which pairs of residues to include in structural alignment. These pairs were fit by a least-squares algorithm, which

minimizes the distance between corresponding pairs of backbone atoms (Kabsch, 1976), and is implemented in the PAP package (Callahan et al., 1990).

To define equivalent residues (Figs. 2B, 3B), we carried out cycles of visual inspection and least-squares alignment. Structurally equivalent residues were initially defined as stretches of four or more consecutive residues with $C\alpha$ separations of less than 3.0 Å in the two overlaid models. Cycles of structural overlay followed by selection of equivalent residues were repeated until a self-consistent solution was found. Finally, additional residues with similar conformations, and separated by less than 5 Å, were added to extend the equivalent segments.

Characterization of surfaces and interfaces

QUANTA programs were used to calculate buried surface areas and accessible surface areas. Computations of the properties of the interface between the [2Fe-2S] and FNR-like interfaces in PDR included the bridging solvents (Fig. 4). The fraction of the buried surface consisting of hydrophilic groups was 0.58 in this case.

Electrostatics calculations

The QDIFFXXS version of the DelPhi program (Nicholls & Honig, 1991), which uses finite difference methods to solve the Poisson-Boltzmann equations for electrostatic potentials at positions on a three-dimensional grid, was employed for calculation of electrostatic potentials at the positions of the 12 non-hydrogen atoms constituting the $Fe_2S_2Cys_4$ cluster (Fe, S^{2-} , $S\gamma$, and $C\beta$). The electrostatic potentials at the cluster (target) atoms, generated by other protein charges, were computed with the charges of Fe, S^{2-} , and cysteine ligand side chains set to 0.0. The ionic strength was held at 0.150; the dielectric constant was set to 4.0 inside the protein and to 80.0 outside the protein. Protein boundaries were determined by DelPhi from the Lee and Richards (Richards, 1985) algorithm using a probe of 1.4 Å radius, and salt ions were excluded from a 2-Å layer around the protein.

Protein charges and partial charges were from the X-PLOR/CHARMM set 11.PRO. Backbone charges in this set are: $C\alpha$, 0.10; N, -0.35; H, 0.25; C, 0.55; and O, -0.55. Polar hydrogens were added to the coordinate lists for Fd using the H-build feature of X-PLOR, and were refined with explicit H-bonding potentials, keeping heavy atoms fixed (Brünger, 1992). The hydrogen attached to $O\gamma$ of Thr 48 of ferredoxin was positioned manually. Hydrogens in PDR were refined with the same explicit H-bonding potentials.

The changes in electrostatic interaction energies, resulting from reduction of the cluster, were calculated from the formula $\sum \Delta q_{i;c^*} \Phi_i$, where Δq_i is the change in the charge at atom i and the sums were taken over the cluster atoms. Charges for the atoms in oxidized and reduced $[Fe_2S_2(SR)_4]$ are from Chen et al. (1993) and L. Noodle-

man (pers. comm.) for model systems where $R = CH_3$. These are based on electrostatic potential charge fits to quantum mechanical calculations using density functional methods for iron-sulfur clusters (Noddleman & Baerends, 1984; Noddleman et al., 1985; Noddleman & Case, 1992). The Δq (reduced - oxidized) values used to compute interactions were: Cys $C\beta$ (1, 2), -0.049; Cys $S\gamma$ (1, 2), -0.214; Cys $C\beta$ (3, 4), -0.028; Cys $S\gamma$ (3, 4), -0.141; S^{2-} , -0.166; Fe1, 0.057; Fe2, 0.146. The cysteine subscripts refer to relative positions along the sequence, and Fe1 is the iron atom that is assumed to accept an electron.² The charge assigned to the iron atoms actually increases slightly on reduction of the cluster, and most of the added negative charge resides on the sulfur atoms. This calculation assumes that reduction is not accompanied by changes in atomic coordinates. In a control calculation using the coordinates for reduced PDR, the electrostatic interaction energy differs by 0.6 kcal/mol.

For comparison of Fd with the excised domain 236-321 of PDR, the coordinates of Fd were superimposed on the PDR domain, and dummy atoms were added to maintain the same scale of grid intervals/Å in each protein. To estimate variations in potentials resulting from the finite grid spacing, calculations of potentials in Fd were compared with and without the coordinate rotation and translation used to superimpose Fd on PDR, and results of origin translations and of focussing (Nicholls & Honig, 1991) to finer grid intervals were examined. Variations in the interaction energies on the order of 0.5 kcal/mol were found by these comparisons.

Acknowledgments

This research has been supported by grants from the NIH (GM16429 to M.L.L.) and NSF (MCB9112699 to P.A.K.); C.M.B. received support from an NIH National Service Award, GM0723. We are grateful to Dr. H.M. Holden for refined coordinates for *Anabaena 7120* ferredoxin, and for comments and discussions. Dr. L. Noddleman kindly communicated his values for the charges of $Fe_2S_2Cys_4$ cluster atoms. We thank Anita Metzger for assistance in preparation of the figures, which were generated using the program MAXIM, obtained from Mark Rould.

References

- Aliverti, A., Jansen, T., Zanetti, G., Ronchi, S., Herrmann, R.G., & Curti, B. (1990). Expression in *Escherichia coli* of ferredoxin-NADP⁺ reductase from spinach. Bacterial synthesis of the holo-flavoprotein and of an active enzyme form lacking the first 28 amino acid residues of the sequence. *Eur. J. Biochem.* 191, 551-555.
- Aliverti, A., Piubelli, L., Zanetti, G., Lübbertedt, T., Herrmann, R.G., & Curti, B. (1993). The role of cysteine residues of spinach ferredoxin-NADP⁺ reductase as assessed by site-directed mutagenesis. *Biochemistry* 32, 6374-6380.
- Andrews, S.C., Shipley, D., Keen, J.N., Findlay, J.B.C., Harrison, P.M., & Guest, J.R. (1992). The hemoglobin-like protein (HMP) of *Escherichia coli* has ferrisiderophore reductase activity and its C-terminal domain shares homology with ferredoxin NADP⁺ reductases. *FEBS Lett.* 302, 247-252.
- Backes, G., Mino, Y., Loehr, T.M., Meyer, T.E., Cusanovich, M.A.,

- Sweeney, W.V., Adman, E.T., & Sanders-Loehr, J. (1991). The environment of Fe₄S₄ clusters in ferredoxins and high-potential iron proteins. New information from X-ray crystallography and resonance Raman spectroscopy. *J. Am. Chem. Soc.* 113, 2055-2064.
- Batie, C.J. & Ballou, D.P. (1987). Electron transfer kinetics of phthalate oxygenase reductase, an iron-sulfur center containing flavoprotein. In *Flavins and Flavoproteins 1987* (Edmondson, D.E. & McCormick, D.B., Eds.), pp. 377-380. Walter de Gruyter & Co., Berlin.
- Batie, C.J. & Kamin, H. (1981). The relation of pH and oxidation-reduction potential to the association state of the ferredoxin-ferredoxin:NADP⁺ reductase complex. *J. Biol. Chem.* 256, 7756-7763.
- Batie, C.J. & Kamin, H. (1984). Electron transfer by ferredoxin:NADP⁺ reductase. Rapid reaction evidence for participation of a ternary complex. *J. Biol. Chem.* 259, 11976-11985.
- Batie, C.J. & Kamin, H. (1986). Association of ferredoxin NADP⁺ reductase with NADP(H): Specificity and oxidation-reduction properties. *J. Biol. Chem.* 261, 11214-11223.
- Bocanegra, J.A., Scrutton, N., & Perham, R.N. (1993). Creation of an NADP-dependent pyruvate dehydrogenase multienzyme complex by protein engineering. *Biochemistry* 32, 2737-2740.
- Bredt, D.S., Hwang, P.M., Glatt, C.E., Lowenstein, C., Reed, R.R., & Snyder, S.H. (1991). Cloned and expressed nitric oxide synthase structurally resembles cytochrome P-450 reductase. *Nature* 351, 714-718.
- Brunel, F. & Davison, J. (1988). Cloning and sequencing of *Pseudomonas* genes encoding vanillate demethylase. *J. Bacteriol.* 170, 4924-4930.
- Brünger, A.T. (1992). *X-PLOR Manual, Version 3.0*. Yale University, New Haven, Connecticut.
- Brünger, A.T., Kruckowski, A., & Erickson, J.W. (1990). Slow-cooling protocols for crystallographic refinement by simulated annealing. *Acta Crystallogr.* A46, 585-593.
- Callahan, T., Gleason, W.B., & Lybrand, T.P. (1990). PAP: A protein analysis package. *J. Appl. Crystallogr.* 23, 434-436.
- Cambillau, C. & Horjales, E. (1987). TOM: A FRODO superpackage for protein-ligand fitting with interactive energy minimization. *J. Mol. Graphics* 5, 174-177.
- Cammack, R. (1992). Iron-sulfur clusters in enzymes—Themes and variations. *Adv. Inorg. Chem.* 38, 281-322.
- Carter, C.W., Jr. (1977). New stereochemical analogies between iron-sulfur electron transport proteins. *J. Biol. Chem.* 252, 7802-7811.
- Carter, C.W., Jr., Kraut, J., Freer, S.T., Alden, R.A., Sieker, L.C., Adman, E., & Jensen, L.H. (1972). A comparison of Fe₄S₄ clusters in high-potential iron protein and in ferredoxin. *Proc. Natl. Acad. Sci. USA* 69, 3526-3529.
- Chan, T.-M., Ulrich, E.L., & Markley, J.L. (1983). Nuclear magnetic resonance studies of two-iron-two-sulfur ferredoxins. 4. Interactions with redox partners. *Biochemistry* 22, 6153-6157.
- Chen, J.L., Mouesca, J.-M., Noodleman, L., Case, D.A., & Bashford, D. (1993). Density functional calculations of redox potentials for FeS clusters including solvation effects. *J. Inorg. Chem.* 51, 449.
- Chothia, C. & Lesk, A. (1986). The relation between the divergence of sequence and structure in proteins. *EMBO J.* 5, 823-826.
- Coglan, V.M. & Vickery, L.E. (1991). Site-specific mutations in human ferredoxin that affect binding to ferredoxin reductase and cytochrome P450ccc. *J. Biol. Chem.* 266, 18606-18612.
- Correll, C.C. (1992). Structure determination and analysis of an iron-sulfur flavoprotein: Phthalate dioxygenase reductase. Ph.D. Dissertation, The University of Michigan, Ann Arbor.
- Correll, C.C., Batie, C.J., Ballou, D.P., & Ludwig, M.L. (1992). Phthalate dioxygenase reductase: A modular structure for electron transfer from pyridine nucleotides to [2Fe-2S]. *Science* 258, 1604-1610.
- De Pascalis, A.R., Jelesarov, I., Ackermann, F., Koppenol, W.H., Hirasawa, M., Knaff, D.B., & Bosshard, H.R. (1993). Binding of ferredoxin to ferredoxin:NADP⁺ reductase: The role of carboxyl groups, electrostatic surface potential, and molecular dipole moment. *Protein Sci.* 2, 1126-1135.
- Dugad, L.B., La Mar, G.N., Banci, L., & Bertini, I. (1990). Identification of localized redox states in plant-type two-iron ferredoxins using the nuclear Overhauser effect. *Biochemistry* 29, 2263-2271.
- Dunham, W.R., Palmer, G., Sands, R.H., & Bearden, A.J. (1971). On the structure of the iron-sulfur complex in the two-iron ferredoxins. *Biochim. Biophys. Acta* 253, 373-384.
- Eggink, G., Engel, H., Vriend, G., Terpstra, P., & Witholt, B. (1990). Rubredoxin reductase of *Pseudomonas oleovorans*. Structural relationship to other flavoprotein oxidoreductases based on one NAD and two FAD fingerprints. *J. Mol. Biol.* 212, 135-142.
- Fukuyama, K., Hase, T., Matsumoto, S., Tsukihara, T., Katsube, Y., Tanaka, N., Kakudo, M., Wada, K., & Matsubara, H. (1980). Structure of *S. platensis* [2Fe-2S] ferredoxin and evolution of chloroplast-type ferredoxins. *Nature* 286, 522-524.
- Gilson, M.K. & Honig, B. (1988a). Energetics of charge-charge interactions in proteins. *Proteins Struct. Funct. Genet.* 3, 32-52.
- Gilson, M.K. & Honig, B. (1988b). Calculations of the total electrostatic energy of a macromolecular system: Solvation energies, binding energies, and conformational analysis. *Proteins Struct. Funct. Genet.* 4, 7-18.
- Gunner, M.R. & Honig, B. (1991). Electrostatic control of midpoint potentials in the cytochrome subunit of the *Rhodopseudomonas viridis* reaction center. *Proc. Natl. Acad. Sci. USA* 88, 9151-9155.
- Gurbel, R.J., Batie, C.J., Sivaraga, M., True, A.E., Fee, J.A., Hoffman, B.M., & Ballou, D.B. (1989). Electron-nuclear double resonance spectroscopy of ¹⁵N-enriched phthalate dioxygenase from *Pseudomonas cepacia* proves that two histidines are coordinated to the [2Fe-2S] Rieske-type clusters. *Biochemistry* 28, 4861-4871.
- Hall, L.H., Bowers, M.L., & Durfor, C.N. (1987a). Further consideration of flavin coenzyme biochemistry afforded by geometry-optimized molecular orbital calculations. *Biochemistry* 26, 7401-7409.
- Hall, L.H., Orchard, B.J., & Tripathy, S.K. (1987b). The structure and properties of flavins: Molecular orbital study based on totally optimized geometries. I. Molecular orbital structure and electron distribution. *Int. J. Quant. Chem.* XXXI, 217-242.
- Haniu, M., McManus, M.E., Birkett, D.J., Lee, T.D., & Shively, J.E. (1989). Structural and functional analysis of NADPH-cytochrome P-450 reductase from human liver: Complete sequence of human enzyme and NADPH-binding sites. *Biochemistry* 28, 8639-8645.
- Hendrickson, W.A. (1985). Stereochemically restrained refinement of macromolecular structures. *Methods Enzymol.* 115, 252-270.
- Huang, Y.Y., Hsu, D.K., & Kimura, T. (1983). The effect of pH on the formal reduction potential of adrenodoxin in the presence and absence of adrenodoxin reductase: The implication in the electron transfer mechanism. *Biochem. Biophys. Res. Commun.* 115, 116-122.
- Hurley, J.K., Salamon, Z., Meyer, T.E., Fitch, J., Cusanovich, M.A., Markley, J., Cheng, H., Xia, B., Chae, Y.K., Medina, M., Gomez-Moreno, C., & Tollin, G. (1993). Amino acid residues in *Anabaena* ferredoxin crucial to interaction with ferredoxin-NADP⁺ reductase: Site-directed mutagenesis and laser flash photolysis. *Biochemistry* 32, 9346-9354.
- Hyde, G.E., Crawford, N.M., & Campbell, W.H. (1991). The sequence of squash NADH:nitrate reductase and its relationship to the sequences of other flavoprotein oxidoreductases. *J. Biol. Chem.* 266, 23542-23547.
- Iyanagi, T. (1977). Redox properties of microsomal reduced nicotinamide adenine dinucleotide-cytochrome *b*₅ reductase and cytochrome *b*₅. *Biochemistry* 16, 2725-2730.
- Iyanagi, T., Makine, N., & Mason, H.S. (1974). Redox properties of the reduced nicotinamide adenine dinucleotide-cytochrome P-450 and reduced nicotinamide adenine dinucleotide-cytochrome *b*₅ reductases. *Biochemistry* 13, 1701-1710.
- Janin, J. & Chothia, C. (1990). The structure of protein-protein recognition sites. *J. Biol. Chem.* 265, 16027-16030.
- Janin, J., Miller, S., & Chothia, C. (1988). Surface, subunit interfaces and interior of oligomeric proteins. *J. Mol. Biol.* 204, 155-164.
- Kabsch, W. (1976). A solution for the best rotation to relate two sets of vectors. *Acta Crystallogr.* A32, 922-923.
- Kabsch, W. & Sander, C. (1983). Dictionary of protein secondary structure: Pattern recognition of hydrogen-bonding and geometrical features. *Biopolymers* 22, 2577-2637.
- Karplus, P.A. (1991). Structure/function of spinach ferredoxin:NADP⁺ oxidoreductase. In *Flavins and Flavoproteins 1990* (Curti, B., Ronchi, S., & Zanetti, G., Eds.), pp. 449-455. Walter de Gruyter & Co., Berlin.
- Karplus, P.A., Daniels, M.J., & Herriott, J.R. (1991). Atomic structure of ferredoxin-NADP⁺ reductase: Prototype for a structurally novel flavoenzyme family. *Science* 251, 60-66.
- Karplus, P.A. & Schulz, G.E. (1989). Substrate binding and catalysis

- by glutathione reductase as derived from refined enzyme: Substrate crystal structures at 2 Å resolution. *J. Mol. Biol.* 210, 163–180.
- Karplus, P.A., Walsh, K.A., & Herriott, J.R. (1984). Amino acid sequence of spinach ferredoxin:NADP⁺ oxidoreductase. *Biochemistry* 23, 6576–6583.
- Kay, C.J., Barber, M.J., Notton, B.A., & Solomonson, L.P. (1989). Oxidation-reduction midpoint potentials of the flavin, haem, and Mopterin centres in spinach nitrate reductase. *Biochem. J.* 263, 285–287.
- Keirns, J.J. & Wang, J.H. (1972). Studies on nicotinamide adenine dinucleotide phosphate reductase of spinach chloroplasts. *J. Biol. Chem.* 247, 7374–7382.
- Langen, R., Jensen, G.M., Jacob, U., Stephens, P., & Warshel, A. (1992). Protein control of iron-sulfur cluster redox potentials. *J. Biol. Chem.* 267, 25625–25627.
- Lindqvist, Y. (1989). Refined structure of spinach glycolate oxidase at 2 Å resolution. *J. Mol. Biol.* 209, 151–166.
- Liu, R. & Zylstra, G. (1992). Cloning and characterization of the genes for phthalate degradation from *Pseudomonas cepacia* DB01. *Abstr. Annu. Meet. Am. Soc. Microbiol.* 1992, 262.
- Ludwig, M.L. & Luschinsky, C.L. (1992). Structure and redox properties of clostridial flavodoxin. In *Chemistry and Biochemistry of Flavoenzymes*, Vol. 3 (Müller, F., Ed.), pp. 427–466. CRC Press, Boca Raton, Florida.
- Lund, J. & Dalton, H. (1985). Further characterisation of the FAD and Fe₂S₂ redox centres of component C, the NADH:acceptor reductase of the soluble methane monooxygenase of *Methylococcus capsulatus* (Bath). *Eur. J. Biochem.* 147, 291–296.
- Markley, J.L., Chan, T.-M., Krishnamoorthi, R., & Ulrich, E.L. (1986). Nuclear magnetic resonance studies of structure-function relationships in iron-sulfur proteins. In *Iron-Sulfur Protein Research* (Matsumura, H., Ed.), pp. 167–181. Japan Scientific Societies Press, Tokyo.
- Massey, V. & Ghisla, S. (1974). Role of charge transfer interactions in flavoprotein catalysis. *Ann. N.Y. Acad. Sci.* 277, 446–465.
- Massey, V., Matthews, R., Foust, G.P., Howell, L.G., Williams, C.H., Jr., Zanetti, G., & Ronchi, S. (1970). A new intermediate in TPNH-linked flavoproteins. In *Pyridine Nucleotide-Dependent Dehydrogenases* (Sund, H., Ed.), pp. 393–411. Springer-Verlag, Berlin.
- Mathews, F.S. (1991) New flavoenzymes. *Curr. Opin. Struct. Biol.* 1, 954–967.
- Matsubara, H. & Hase, T. (1983). Phylogenetic consideration of ferredoxin sequences in plants, particularly algae. In *Protein and Nucleic Acids in Plant Systematics* (Jensen, U. & Fairbrothers, D.E., Eds.), pp. 168–181. Springer-Verlag, Berlin.
- Mattevi, A., Obmolova, G., Sokatch, J.R., Betzel, C., & Hol, W.J.G. (1992). The refined crystal structure of *Pseudomonas putida* lipamide dehydrogenase complexed with NAD⁺ at 2.45 Å resolution. *Proteins Struct. Funct. Genet.* 13, 336–351.
- Neidle, E.L., Hartnett, C., Orntston, L.N., Bairoch, A., Rekik, M., & Harayama, S. (1991). Nucleotide sequences of the *Acinetobacter calcoaceticus* benABC genes for benzoate 1,2-dioxygenase reveal evolutionary relationships among multicomponent oxygenases. *J. Bacteriol.* 173, 5385–5395.
- Nicholls, A. & Honig, B. (1991). A rapid finite difference algorithm, utilizing successive over-relaxation to solve the Poisson-Boltzmann equation. *J. Comp. Chem.* 12, 435–445.
- Noodleman, L. & Baerends, E.J. (1984). Electronic structure, magnetic properties, ESR, and optical spectra for 2-Fe ferredoxin models by LCAO-Xα valence bond theory. *J. Am. Chem. Soc.* 106, 2316–2327.
- Noodleman, L. & Case, D.A. (1992). Density functional theory of spin polarization and spin coupling in iron-sulfur clusters. *Adv. Inorg. Chem.* 38, 423–470.
- Noodleman, L., Norman, J.G., Jr., Osborne, J.H., Aizman, A., & Case, D.A. (1985). Models for ferredoxins: Electronic structures of iron-sulfur clusters with one, two, and four iron atoms. *J. Am. Chem. Soc.* 107, 3418–3426.
- Nordlund, I., Powłowski, J., & Shingler, V. (1990). Complete nucleotide sequence and polypeptide analysis of multicomponent phenol hydroxylase from *Pseudomonas* sp. strain CF600. *J. Bacteriol.* 171, 6826–6833.
- Ostrowski, J., Barber, M.J., Rueger, D.C., Miller, B.E., Siegel, L.M., & Kredich, N.M. (1989). Characterization of the flavoprotein moieties of NADPH-sulfite reductase from *Salmonella typhimurium* and *Escherichia coli*. Physicochemical and catalytic properties, amino acid sequence deduced from DNA sequence of cysJ, and comparison with NADPH-cytochrome P-450 reductase. *J. Biol. Chem.* 264, 15796–15808.
- Pai, E.F., Karplus, P.A., & Schulz, G.E. (1988). Crystallographic analysis of the binding of NADPH, NADPH fragments, and NADPH analogues to glutathione reductase. *Biochemistry* 27, 4465–4474.
- Poe, M., Phillips, W.D., Glickson, J.D., McDonald, C.C., & San Pietro, A. (1970). Proton magnetic resonance studies of the ferredoxins from spinach and parsley. *Proc. Natl. Acad. Sci. USA* 68, 68–71.
- Prosser, I.M. & Lazarus, C.M. (1990). Nucleotide sequence of a spinach nitrate reductase cDNA. *Plant Mol. Biol.* 15, 187–190.
- Pueyo, J.J., Concepcion, R., Mayhew, S.G., & Gomez-Moreno, C. (1992). Complex formation between ferredoxin and ferredoxin-NADP⁺ reductase from *Anabaena* PCC 7119: Cross-linking studies. *Arch. Biochem. Biophys.* 294, 367–372.
- Pueyo, J.J., Gomez-Moreno, C., & Mayhew, S.G. (1991). Oxidation-reduction potentials of ferredoxin-NADP⁺ reductase and flavodoxin from *Anabaena* PCC 7119 and their electrostatic and covalent complexes. *Eur. J. Biochem.* 202, 1065–1071.
- Rayment, I., Wesenberg, G., Meyer, T.E., Cusanovich, M.A., & Holden, H.M. (1992). Three-dimensional structure of the high-potential iron-sulfur protein isolated from the purple phototrophic bacterium *Rhodocyclus tenuis* determined and refined at 1.5 Å resolution. *J. Mol. Biol.* 228, 672–686.
- Richards, F.M. (1985). Calculations of molecular volumes and areas for structures of known geometry. *Methods Enzymol.* 115, 440–464.
- Rypniewski, W.R., Breiter, D.R., Benning, M.M., Wesenberg, G., Oh, B.-H., Markley, J.L., Rayment, I., & Holden, H.M. (1991). Crystallization and structure determination to 2.5 Å resolution of the oxidized [2Fe-2S] ferredoxin isolated from *Anabaena* 7120. *Biochemistry* 30, 4126–4131.
- Salmeen, I. & Palmer, G. (1972). Contact-shifted NMR of spinach ferredoxin: Additional resonances and partial assignments. *Arch. Biochem. Biophys.* 150, 767–773.
- Schulz, G.E. (1992). Binding of nucleotides by proteins. *Curr. Opin. Struct. Biol.* 2, 61–67.
- Scrutton, N.S., Berry, A., & Perham, R.N. (1990). Redesign of the coenzyme specificity of a dehydrogenase by protein engineering. *Nature* 343, 38–43.
- Segal, A.W., West, I., Wientjes, F., Nugent, J.H.A., Chavan, A.J., Haley, B., Garcia, R.C., Rosen, H., & Scrace, G. (1992). Cytochrome b₂₄₅ is a flavocytochrome containing FAD and the NAPH-binding site of the microbicidal oxidase of phagocytes. *Biochem. J.* 284, 781–788.
- Sharp, K. & Honig, B. (1990). Calculating total electrostatic energies with the nonlinear Poisson-Boltzmann equation. *J. Phys. Chem.* 94, 7684–7692.
- Shirabe, K., Yubisui, T., Nishino, T., & Takeshita, M. (1991). Role of cysteine residues in human NADH-cytochrome b₅ reductase studied by site-directed mutagenesis. *J. Biol. Chem.* 266, 7531–7536.
- Simon, M.J., Osslund, T.D., Saunders, R., Ensley, B.D., Suggs, S., Harcourt, A., Suen, W.-C., Cruden, D.L., Gibson, D.T., & Zylstra, G.J. (1993). Sequences of genes encoding naphthalene dioxygenase in *Pseudomonas putida* strains G7 and NCIB 9816-4. *Gene* 127, 31–37.
- Skjeldal, L., Westler, W.M., Oh, B.-H., Krezel, A.M., Holden, H.M., Jacobson, B.L., Rayment, I., & Markley, J.L. (1991). Two-dimensional magnetization exchange spectroscopy of *Anabaena* 7120 ferredoxin. Nuclear Overhauser effect and electron self-exchange cross peaks from amino acid residues surrounding the 2Fe-2S cluster. *Biochemistry* 30, 7363–7368.
- Sligar, S.G. & Gunsalus, I.C. (1976). A thermodynamic model of regulation: Modulation of redox equilibria in camphor monooxygenase. *Proc. Natl. Acad. Sci. USA* 73, 1078–1082.
- Soman, K., Yang, A.-S., Honig, B., & Fletterick, R. (1989). Electric potentials in trypsin enzymes. *Biochemistry* 28, 9918–9926.
- Spence, J.T., Barber, M.J., & Solomonson, L.P. (1988). Stoichiometry of electron uptake and oxidation/reduction midpoint potentials of NADH:nitrate reductase. *Biochem. J.* 250, 921–923.
- Spyrou, G., Haggard-Ljungquist, E., Krook, M., Jornvall, H., Nilsson, E., & Reichard, P. (1991). Characterization of the flavin reductase gene (fre) of *Escherichia coli* and construction of a plasmid for overproduction of the enzyme. *J. Bacteriol.* 173, 3673–3679.

- Stainthorpe, A.C., Lees, V., Salmond, G.P.C., Dalton, H., & Murrell, J.C. (1990). The methane monooxygenase gene cluster of *Methylococcus capsulatus* (Bath). *Gene* 91, 27–34.
- Sussman, J.L., Brown, J.H., & Shoham, M. (1986). X-ray structural studies on a salt-loving ferredoxin from *Halobacterium* of the Dead Sea. In *Iron-Sulfur Protein Research* (Matsubara, H., Ed.), pp. 69–82. Japan Scientific Societies Press, Tokyo.
- Suzuki, M., Hayakawa, T., Shaw, J.P., Rekik, M., & Harayama, S. (1991). Primary structure of xylene monooxygenase: Similarities to and differences from the alkane hydroxylation system. *J. Bacteriol.* 173, 1690–1695.
- Swartzman, E., Miyamoto, C., Graham, A., & Meighen, E. (1990). Delination of the transcriptional boundaries of the *lux* operon of *Vibrio harveyi* demonstrates the presence of two new *lux* genes. *J. Biol. Chem.* 265, 3513–3517.
- Swenson, R.P., Krey, D.G., & Eren, M. (1991). The site-directed mutagenesis of bacterial flavodoxins. In *Flavins and Flavoproteins 1990* (Curti, B., Ronchi, S., & Zanetti, G., Eds.), pp. 415–422. Walter de Gruyter & Co., Berlin.
- Tomatsu, S., Kobayashi, Y., Fukumaki, Y., Yubisui, T., Orii, T., & Sakaki, Y. (1989). The organization and the complete nucleotide sequence of the human NADH-cytochrome *b*₅ reductase gene. *Gene* 80, 353–361.
- Tronrud, D.E., Ten Eyck, L.K., & Matthews, B.W. (1987). An efficient general-purpose least-squares program for macromolecular structures. *Acta Crystallogr. A* 43, 489–501.
- Tsukihara, T., Fukuyama, K., Mizushima, M., Harioka, T., Kusunoki, M., Katsume, Y., Hase, T., & Matsubara, H. (1990). Structure of the [2Fe-2S] ferredoxin I from the blue-green alga *Aphanothecace sacrum* at 2.2 Å resolution. *J. Mol. Biol.* 216, 399–410.
- Vieira, B.J., Colvert, K.K., & Davis, D.J. (1986). Chemical modification and cross-linking as probes of regions on ferredoxin involved in its interaction with ferredoxin: NADP reductase. *Biochim. Biophys. Acta* 851, 109–122.
- Werth, M.T., Cecchini, G., Manodori, A., Ackrell, B.A.C., Schröder, I., Gunsalus, R.P., & Johnson, M.K. (1990). Site-directed mutagenesis of conserved cysteine residues in *Escherichia coli* fumarate reductase: Modification of the spectroscopic and electrochemical properties of the [2Fe-2S] cluster. *Proc. Natl. Acad. Sci. USA* 87, 8965–8969.
- Wierenga, R.K., Terpstra, P., & Hol, W.G.J. (1986). Prediction of the occurrence of the ADP-binding $\beta\alpha\beta$ -fold in proteins, using an amino acid sequence fingerprint. *J. Mol. Biol.* 187, 101–107.
- Zanetti, G., Morelli, D., Ronchi, S., Negri, A., Aliverti, A., & Curti, B. (1988). Structural studies on the interaction between ferredoxin and ferredoxin-NADP⁺ reductase. *Biochemistry* 27, 3753–3759.